A METHODOLOGY FOR BUMP DETECTION USING INERTIAL PROFILE MEASUREMENTS

THE UNIVERSITY OF TEXAS AT ARLINGTON
TRANSPORTATION INSTRUMENTATION LABORATORY

RESEARCH REPORT 0-4479-1
Research Project Number 0-4479

Roger S. Walker, Ph.D., P.E
Emmanuel Fernando, Ph.D., P.E.
Yoshitaka Sho, BS, CSE

Date: April 2005

Technical Report Documentation Page

1. Report No.	2. Government Accession No.	3. Recipient's Catalog No.
FHWA/TX-05/0-4479-1		

4. Title and Subtitle	5. Report Date
A Methodology for Bump Detection Using Inertial Profile Measurements	April 2004, revised April 2005
	6. Performing Organization Code

7. Author(s)	8. Performing Organization Report No.
Roger S. Walker, PhD, P.E., Emmanuel Fernando, PhD, P.E., Yoshitaka Sho, BS, CSE	0-4479-1

9. Performing Organization Name and Address	10. Work Unit No. (TRAIS)
The University of Texas at Arlington, Transportation Instrumentation Laboratory	11. Contract or Grant No. 0-4479

12. Sponsoring Agency Name and Address	13. Type of Report and Period Covered
Texas Department of Transportation Research and Technology Implementation Office P. O. Box 5080 Austin, TX 78763-5080	Technical Report 9/1/03 – 8/31/05
	14. Sponsoring Agency Code

15. Supplementary Notes

Project performed in cooperation with the Texas Department of Transportation, Federal Highway Administration.

16. Abstract

The Texas Department of Transportation (TxDOT) started implementing its new ride quality specification in 2002. This specification requires the use of inertial profilers in lieu of profilographs for quality assurance testing of surface smoothness on new construction and rehabilitations projects. The profilograph-based ride specification that it replaced includes criteria on both sections-wide and localized roughness. Although a method is currently used to evaluate localized roughness, its assessment, and that of section-wide roughness is based on different criteria. The new ride specification identifies defects based on an allowable difference between the average measured profile and its moving average, and assesses section-wide roughness using the International Roughness Index (IRI). While both criteria are correlated to user perception of ride quality as measured by the Present Serviceability Index (PSI), this index is not presently used to establish the need for corrections. Also, the improvements in PSI resulting from corrections are neither evaluated nor predicted in the new ride specification. The new equation has been found to be more sensitive to the occurrence of localized roughness than IRI or the current ride equation. Thus, TxDOT initiated Project 4479 to investigate the application of the new equation for detecting defects in a smoothness specification. Its objectives are to determine methods for defining localized roughness characteristics that are objectionable to ride; and establish how these characteristics can be measured in an effective way for construction quality control and assurance using inertial reference profile data. The results of this project is discussed in the report.

17. Key Word	18. Distribution Statement
Smoothness, localized roughness, bump identification bump template, Template Analysis Procedure (TAP).	No restrictions. This document is available to the public through the National Technical Information Service, Springfield, Virginia 22161, www.ntis.gov

19. Security Classif. (of this report)	20. Security Classif. (of this page)	21. No. of Pages	22. Price
Unclassified	Unclassified	86	

A METHODOLOGY FOR BUMP DETECTION USING INERTIAL PROFILE MEASUREMENTS

THE UNIVERSITY OF TEXAS AT ARLINGTON
TRANSPORTATION INSTRUMENTATION
LABORATORY

RESEARCH REPORT 0-4479-1
Research Project Number 0-4479
Project Title: Develop a Methodology for Establishing Bump Detection Using Inertial Profile Measurements for Implementation With the Ride Specification

Roger S. Walker, Ph.D., P.E
Emmanuel Fernando, Ph.D., P.E.
Yoshitaka Sho, BS, CSE

Performed in cooperation with the Texas Department of Transportation and the Federal Highway Administration

Date: April 2005

Notice – The United States Government and the State of Texas do not endorse products or manufacturers. Trade or manufacturers' names appear solely because they are considered essential to the object of the report.

DISCLAIMER(S)

The contents of this report reflect the views of the author(s), who is (are) responsible for the facts and the accuracy of the data presented herein. The contents do not necessarily reflect the official view or policies of the Federal Highway Administration or the Texas Department of Transportation. This report does not constitute a standard, specification, or regulation.

There was no invention or discovery conceived or first actually reduced to practice in the course of or under this contract, including any art, method, process, machine, manufacture, design or composition of matter, or any new useful improvement thereof, or any variety of plant, which is or may be patentable under patent laws of the United States of America or any foreign country.

ACKNOWLEDGEMENTS

The authors would like first to acknowledge Carl Bertrand and David Head of the Texas Department of Transportation. Without their support, this research project would not have been possible. Acknowledgements are also due the students and staff personnel, in particular Eric Becker at the Transportation Instrumentation Laboratory facility at the University of Texas at Arlington.

Table of Contents

List of Figures

List of Tables

Chapter 1
Background on Research Project

1.1 Introduction

The Texas Department of Transportation (TxDOT) started implementing its new ride quality specification in September 2002. This specification requires the use of inertial profilers in lieu of profilographs for quality assurance testing of surface smoothness on new construction and rehabilitation projects. The profilograph-based ride specification that it replaced includes criteria on both section-wide and localized roughness. The new ride quality specification uses the International Roughness Index (IRI) to assess the quality of surface smoothness for each 0.1 mile section of a project. It also uses the average of the measured wheel path profiles to determine the locations of bumps and dips (also referred to as defects in the former profilograph specification).

Although a method is currently used to evaluate localized roughness in the new smoothness specification, its assessment, and that of section-wide roughness, is based on different criteria. The new ride specification identifies defects based on an allowable difference between the average measured profile and its moving average, and assesses section-wide roughness using IRI. While both criteria are correlated to user perception of ride quality as measured by the present serviceability index, PSI is not presently used to establish the need for corrections, nor are the improvements in PSI resulting from corrections evaluated or predicted in the new ride specification. It is from this perspective that the need for Project 0-4479 becomes apparent. In large part, this project is a spin-off from a previous project (0-4901) conducted by Walker and Fernando (2002) that developed a new ride equation for TxDOT. Project 0-4901 aimed to evaluate the adequacy of the existing ride equation in predicting user perception of ride quality, considering that significant changes in vehicle characteristics and pavement construction methods have taken place since its original development. The existing equation is based on data collected from ride surveys conducted in the late 1960s. As will be presented later, researchers found the new ride equation to be more sensitive to the occurrence of localized roughness than IRI

or the existing ride equation. Thus, TxDOT initiated Project 0-4479 to investigate the application of the new ride equation for detecting defects in a smoothness specification. Its objectives are to:

- Determine methods for defining localized roughness characteristics that are objectionable to ride; and
- Establish how these characteristics can be measured in an effective way for construction quality control and assurance using inertial reference profile data.

The method to be developed will provide the locations, widths and amplitudes of unacceptable bumps and dips. The expected advantages of this approach are:

- The evaluation of localized roughness is based on user perception of ride quality. If the smoothness of a pavement section meets or exceeds a specified PSI threshold, its ride quality is deemed acceptable from the road user's perspective. The threshold value may vary depending on highway functional class.
- Since TxDOT uses PSI to assess the ride quality of its highway network for pavement management purposes, using this index as a criterion for evaluating localized roughness would be consistent with the current practice.
- A smoothness specification based on PSI may be established, should TxDOT decide to proceed in this direction. Under this specification, the new ride equation is not only used for evaluating localized roughness but also the acceptability of the section smoothness. The result is a specification that is simpler, based solely on user perception of ride quality and one that provides consistency in the way by which pavement smoothness is measured, from initial construction, through the end of a pavement's life cycle.

To accomplish the objectives of this project, researchers investigated the application of TxDOT's new ride equation for evaluating localized roughness using inertial reference profile measurements. This report focuses on the development of a bump 'template' that can be used for identifying various bump levels for both newly constructed and overlaid pavements.

1.2 Background and Literature Review

A National Quality Initiative (1996) survey identified quality of the roadway surface as the top priority for improving the nation's highways. This opinion of highway

users on the importance of ride quality is shared by state highway agencies, which have increasingly been adopting and implementing smoothness specifications for new construction and rehabilitation. Many of the specifications used are based on the profilograph, although an increasing number of states have begun (or are in the process of) implementing smoothness specifications based on inertial profilers. In 2000, TxDOT introduced a new ride specification that uses IRIs computed from surface profiles for acceptance testing of initial pavement smoothness. Since its introduction, this specification underwent several changes in response to comments provided by TxDOT engineers and industry representatives. Implementation of the new ride specification began in 2002 when TxDOT issued Special Provision and/or Specification Change Memorandum 10-02 approving statewide use of Special Specifications (SS) 5880 (93) and its counterpart, 5440 (95). Researchers note that both specifications are identical, except that SS 5880 is used with the 1993 Texas standard specifications, while SS 5440 is used with the 1995 standard specifications. SS 5880/5440 requires profiles measured with inertial profilers for quality assurance testing of initial pavement smoothness. Engineers use the IRIs computed from surface profiles to evaluate the ride quality of 0.1 mile sections along a given project. In addition, the profiles are used to detect localized roughness following a variation of a procedure proposed by Fernando and Bertrand (2002). This procedure is presented later in this chapter.

Inasmuch as the majority of state highway agencies still use the profilograph for acceptance testing of initial pavement smoothness, the most common procedure for detecting localized roughness is based on the profilograph bump template. These smoothness specifications normally include a requirement that the finished surface should have no bumps greater than 0.3 inches over a base length of 25 ft. Where bumps are detected, the contractor is required to correct the profile at these locations, which typically call for diamond grinding on concrete pavements. In a previous study conducted in Texas, Fernando and Leong (1997) assessed the applicability of a bump requirement in a smoothness specification based on measurements made with inertial profilers. That study included an evaluation of surface profilers that covered van-mounted inertial profilers, lightweight inertial profilers, and profilers referred to as "rolling dipsticks," which provide unfiltered profiles. This evaluation, which TTI

researchers conducted in 1996, aimed to establish the availability of equipment for implementing a profile-based smoothness specification in Texas. It was a comprehensive evaluation that included an assessment of repeatability and accuracy of measured profiles and smoothness statistics determined from profiles. In the same study, researchers fabricated artificial bumps having the heights and base lengths shown in Table 1.1. The bumps were made of silicon rubber and molded with a smooth tapered profile. The artificial bumps were placed at selected intervals along the inside wheel path of a test section. Profile measurements were then taken with various inertial profilers to evaluate the accuracy with which the locations and heights of bumps are determined from these devices.

Figure 1.1 illustrates typical data obtained from all profilers. The figure shows profiles measured with and without the artificial bumps using TxDOT's surface profiler. Observe that the bumps appear distorted in the measured profile as evidenced by the sharp drop in the relative elevations after each bump. This distortion, which is seen as an asymmetry in the bump profile, is an artifact of the filtering. However, between bumps, the profile recovers and gets back on the actual pavement surface, i.e., the profile after the bump eventually merges with the profile measured without the bumps. All inertial profilers tested during the study exhibited this self-correcting capability.

Table 1.2 shows the locations of the bump peaks as determined from the profiles taken with the artificial bumps in place. The locations are referred from the start of the test section. It is observed that the bump locations are very much comparable between the different profilers, indicating that the data from any profiler can be used to locate the bumps placed on the test section. However, it was not possible to get the bump height directly from the profile to compare with the height measured using rod and level. The distortion in the profile immediately after a bump makes it difficult to measure the height as the baseline is skewed. This finding implies that a permissible bump criterion, like the one used in existing profilograph specifications, would be inappropriate to include in a profile-based smoothness specification, without additional data processing to remove the distortion in the bump profile attributed to the filtering inherent in inertial profilers. Alternatively, the profilograph response may be simulated using profile data to detect defects based on the profilograph bump template, as some state highway agencies do. This approach was not used in this

project as it is inconsistent with the research objectives noted previously.

In view of the profile distortion at the vicinity of a bump attributed to filtering, Fernando and Bertrand (2002) proposed a simple method for detecting areas of localized roughness based on the moving average of inertial reference profile data. Figure 1.2 illustrates data from an inertial profiler taken along the inside wheel path of a given pavement.

Table 1.1 Artificial Bumps Used to Evaluate Profiler Response

Bump	Height (in)[1]	Base Length (ft)
1	1.03	4.0
2	0.38	8.0
3	0.91	4.0
4	1.14	2.0
5	1.09	8.0
6	1.35	4.0
7	0.52	2.0

[1] Determined from rod and level after placement of bumps

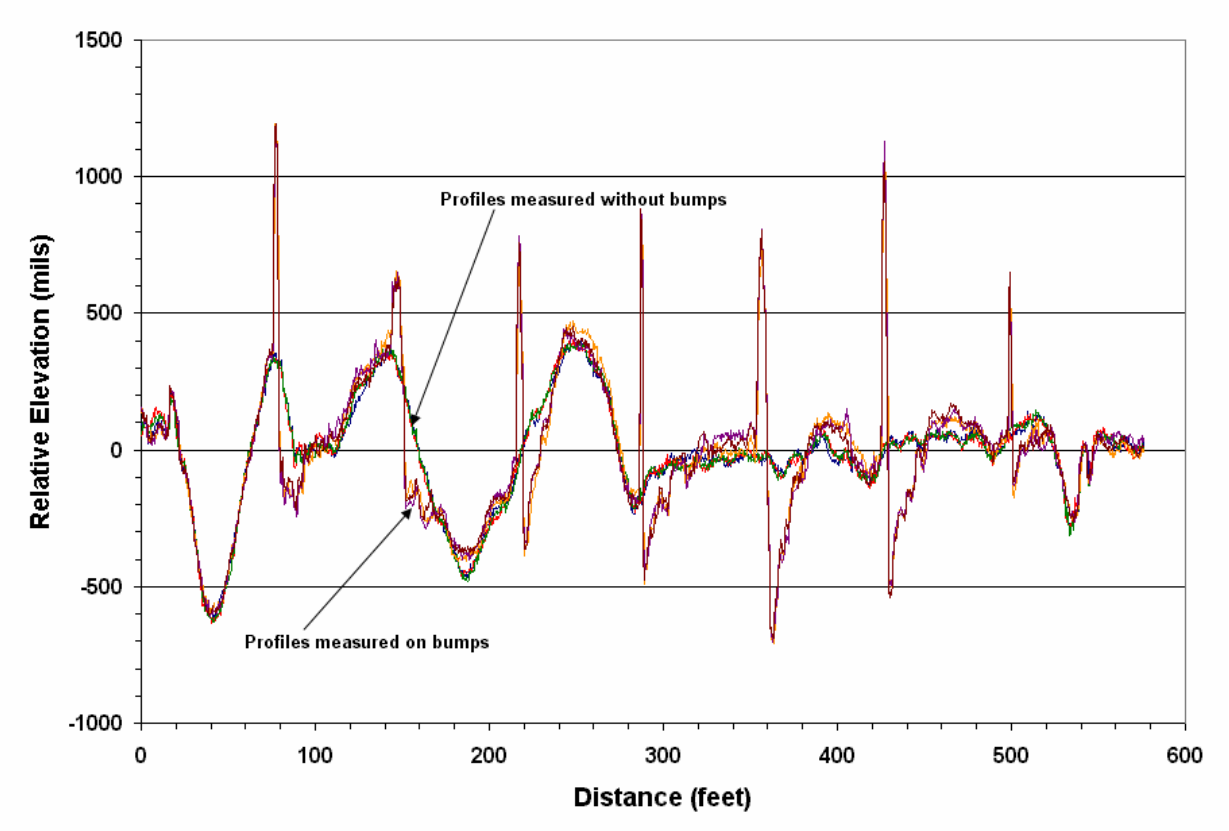

Figure 1.1 Examples of profiles measured with and without the artificial bumps

Table 1.2 Bump locations determined from profile data on artificial bumps

Bump	Location of Bump Peak (ft)				
	Lightweight Profiler			Full-Sized Profiler	
	1	2	3	1	2
1	77.20	78.18	77.00	77.40	77.79
2	146.42	149.80	149.51	147.11	149.90
3	217.13	218.64	217.03	217.75	217.13
4	287.50	288.12	287.70	288.19	287.34
5	357.05	358.60	356.30	357.19	356.43
6	427.43	429.23	427.26	428.22	426.77
7	497.74	502.33	499.74	500.72	499.31

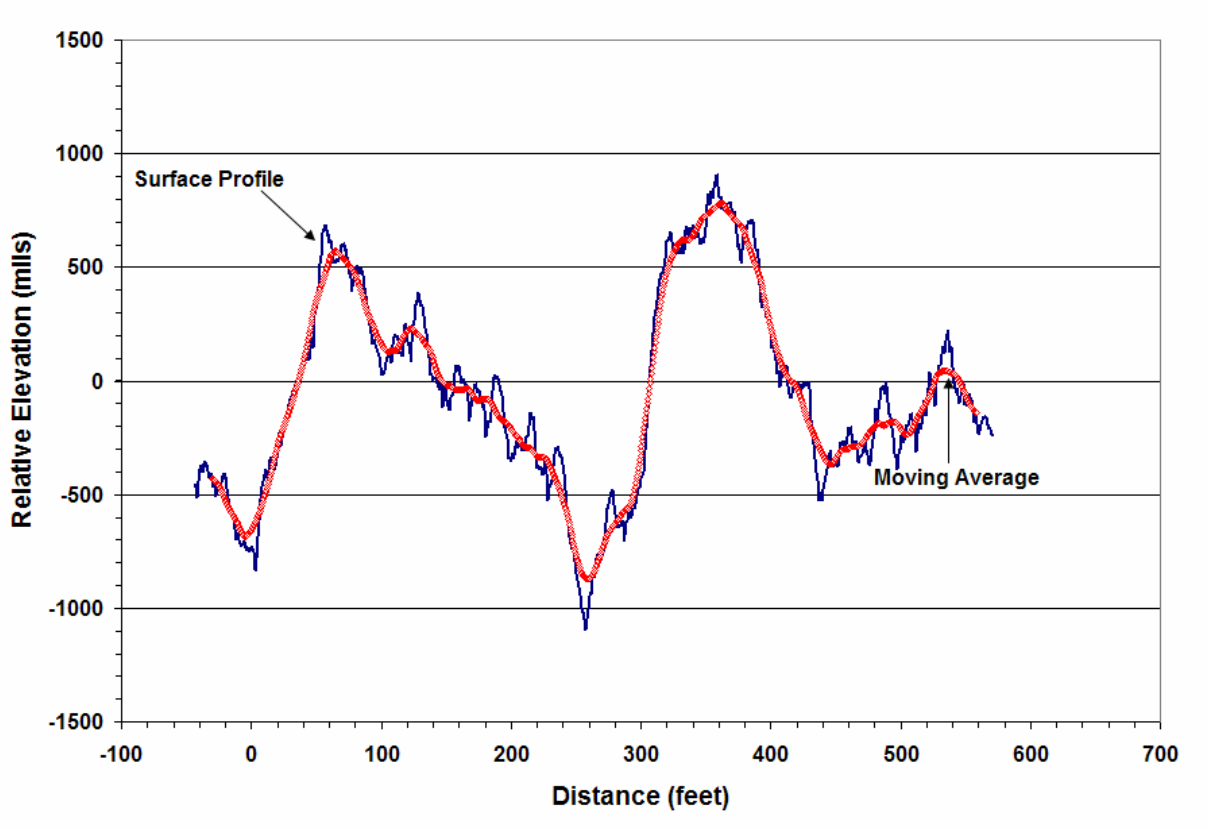

Figure 1.2 Measured and Moving Average Profiles

For the data shown, relative elevations were recorded at 6-inch intervals. The elevations are plotted in Figure 1.2 along with the moving averages determined using a base length of 25 ft.

Figure 1.2 shows locations within the section where the profile significantly deviates from the moving average. For the problem of finding rough areas, a higher deviation from the moving average indicates a greater likelihood of a surface defect at the given location. Fernando and Bertrand (2002) examined the correlation between the deviations of the measured profile from the moving average, and the locations of bumps as determined from a simulation of the profilograph response to the measured profile. The results from this simulation are given in Figure 1.3, which shows the locations of bumps within the section investigated. These bumps are plotted as dots at the top of the figure, where the measured and moving average profiles are also shown. Note that the bumps track the locations of peaks in the measured profile. The peak deviations that coincide with the bump locations ranged from about 134 to 217 mils, with an average deviation of 165 mils from the moving average.

The procedure proposed by Fernando and Bertrand (2002) requires a threshold on the magnitude of the deviation from the moving average to identify potential must-grind locations. This threshold corresponds to the minimum amplitude of a potential defect. Note that not every deviation exceeding the threshold corresponds to the peak of a bump (or trough of a dip). That location may be part of a bump, but not necessarily its peak. The location of the peak must be determined as part of the algorithm for detecting localized roughness.

Based on the limited data presented in their paper, Fernando and Bertrand suggested 150 mils as a reasonable threshold, but noted that further analyses of profile data are necessary to establish this parameter more firmly. The authors also point out that the threshold is simply used to identify potential must-grind locations. The actual identification of localized rough areas is based on the projected decrease in the section roughness if these potential must-grind locations are corrected or removed from the profile.

It is noted that a variation of the above method is implemented for quality assurance testing of initial smoothness in TxDOT's new ride specification. In this implementation, the moving average is calculated using the average of the wheel path profiles, in lieu of evaluating each wheel path. Differences between the average

profile and its moving average are then determined, and deviations exceeding 150 mils are flagged as localized rough areas in SS5880/5440. In a subsequent re-write of

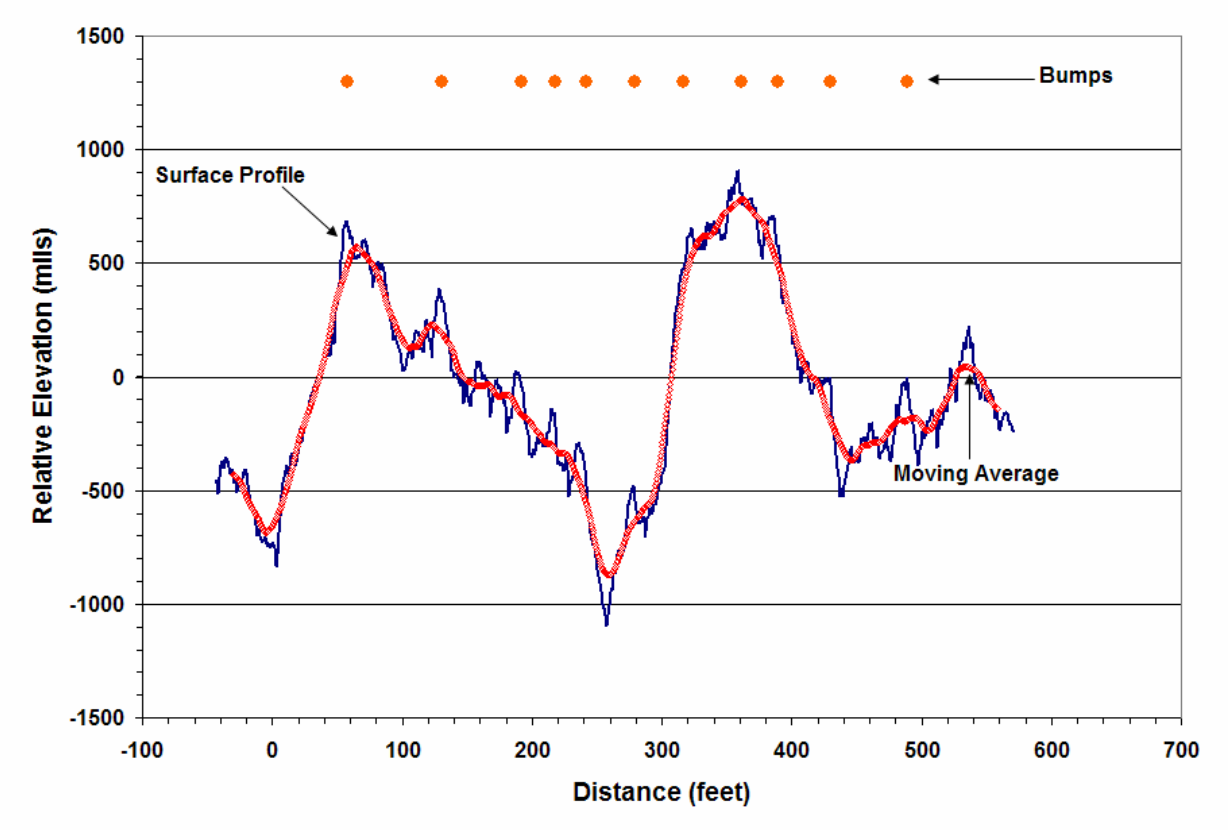

Figure 1.3 Bump Locations from Profilograph Simulation vs. Peak Deviations

the standard ride specification, TxDOT added a bump penalty gap as a criterion for detecting localized roughness. This new specification, designated as Item 585, is included in TxDOT's 2004 standard specifications. It incorporates additional revisions made to SS5880/5440 by TxDOT's specification review committee. Item 585 specifies a bump penalty gap of 5 ft, i.e., no more than one occurrence of localized roughness is assessed for every 5 ft of longitudinal distance.

1.3 Report Coverage

This report documents the research conducted to develop a methodology for evaluating localized roughness from inertial reference profile measurements. Chapter 1 presents the objectives of the project, explains its significance to the existing

practice of evaluating initial pavement smoothness, and reviews the existing method of detecting localized roughness in TxDOT's new ride specification. Inasmuch as TxDOT's new ride equation provides the basis for the methodology developed in this current project, Chapter 2 begins with a description of this new equation, which was developed in Project 0-4901. It then illustrates the sensitivity of this equation to the presence of defects using profile data collected on in-service pavements. In addition, Chapter 2 presents the methods considered for using the new ride equation to detect localized roughness. The selected method, referred to as template analysis, is developed in Chapter 3. Chapter 4 uses the criteria for identifying defects discussed in Chapter 3 on profile data collected from a TxDOT project, and compares these results with the existing method implemented in TxDOT's new ride specification. Finally, Chapter 5 summarizes the findings from the research project and provides recommendations for implementation efforts. The appendix documents work conducted by researchers to collect profile data on projects for developing the procedure to detect localized roughness.

Chapter 2

Localized Roughness and the New Ride Equation

2.1 Introduction

As noted in Chapter 1, a new ride equation developed in the TxDOT Project 0-4901 played an important role in this current research of developing procedures for identifying localized roughness. The new ride equation, which is a function of the profile wavelengths, is used to predict ride by correlating the amplitudes of these wavelengths to panel ratings. The ride survey used to obtain the panel ratings was conducted in Texas in 1999 and 2000. It was during the verification of this ride equation when it appeared that the new ride model might also be useful to aid in the identification procedures for localized roughness.

The motivation of using spectral estimates of road profile data for predicting ride occurred after grouping the sections according to present serviceability ratings (PSRs) from raters and then computing the average power spectral estimates for all profile runs for each of the PSR groups. This grouping is shown in Figure 2.1 for each of the frequency bands.

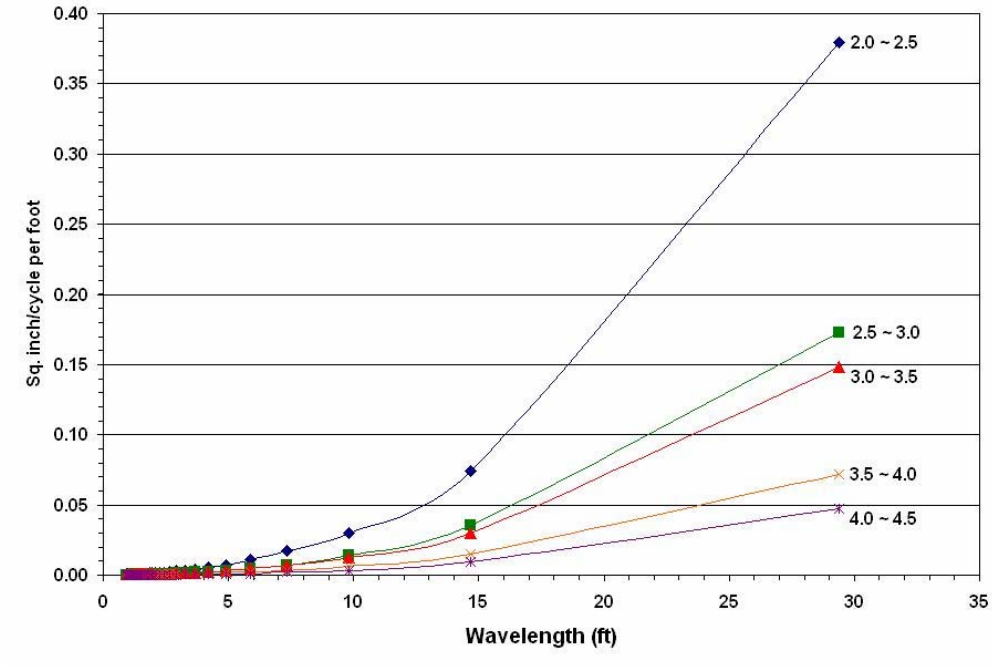

Figure 2.1 Wavelength vs. Power Spectral Rating from Project 4901 Ride Surveys

As noted in this plot, there appears to be a relationship between the spectral components and the average ride ratings of the rating panel (PSR). Using a combination of various signal processing and regression analysis methods the following ride model was developed**:**

$$PSI = 5\, e^{-\alpha P} \qquad (2.1)$$

where, PSI denotes the predicted PSR and αP can be described as follows.

$$\alpha P = \alpha_0 + \alpha_1 P_1 + \alpha_2 P_2 + \ldots + \alpha_8 P_8 \qquad (2.2)$$

$$\alpha P = \alpha_1 \sqrt{P_1} + \alpha_2 \sqrt{P_2} + \ldots\ldots + \alpha_8 \sqrt{P_8}$$

and where each *P* term represents a power spectrum for each frequency components, 1/8, 2/8, 3/8, 4/8, 5/8, 6/8, 7/8, and one cycle per meter.

Using the Discrete Fourier Transform (DFT), the power spectrum for any frequency, f, is computed in accordance with the equation 2.3 from which the power spectral estimates can be determined.

$$X(m) = \sum_{k=0}^{N-1} x_k e^{-j2*pi*k*f*m}, \quad 0 \le f \le \frac{1}{2T} \qquad (2.3)$$

2.2 The New Ride Equation as an Indicator of Localized Roughness

Unlike the current ride equation that is a direct function of IRI, the new equation relates user ride opinions to the physical wavelength characteristics of the associated pavement profile. During the evaluation of the new ride equation in project 4901, a number of comparisons between the current and new ride equation were made. In September of 2001, during a repeat verification of this equation on profiles collected from the Austin Test Sections, one section was found to be significantly different than noted in previous measurements. In all earlier comparisons, the new ride equation typically provided somewhat lower SI readings for smooth pavements and higher readings for the rough sections. These differences were for the most part never

greater than 0.5 SI. Figure 3.2 illustrates the comparisons based on the 2001 data runs.

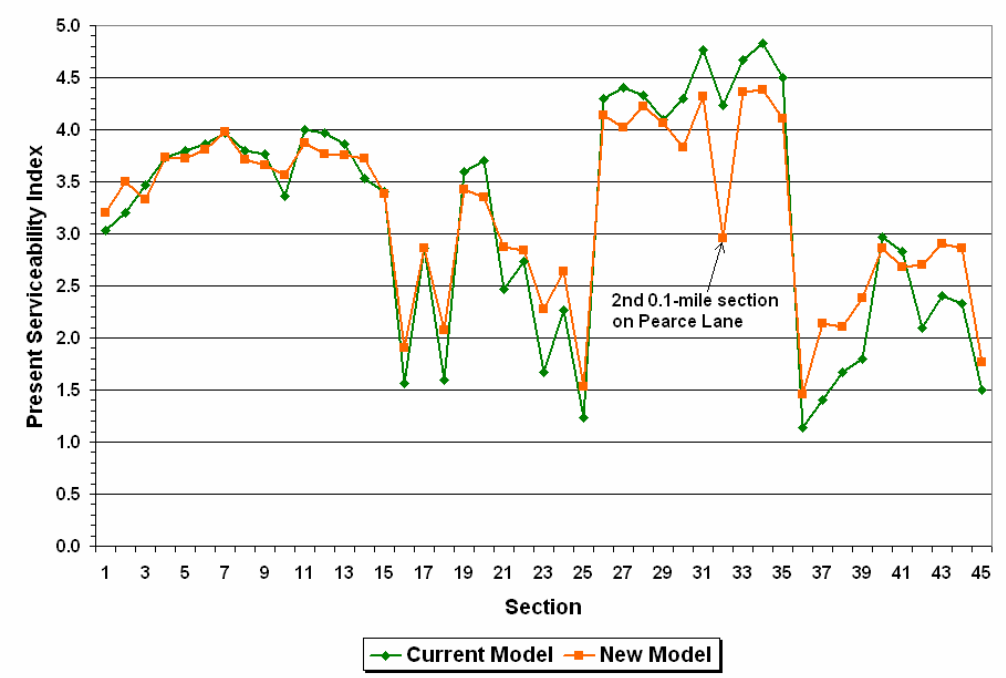

Figure 2.2 Comparisons between Current and New SI Models on Austin Test Sections

As noted in the figure, the SIs computed between the current and new model on the second 0.1 mile section of Pearce Lane were significantly different (4.2 vs. 3.0) and had changed from a previous reading of 4.26 in less than three months. In further investigations, it was found that a pothole had formed in the left wheel path of this section (see Figure 2.3). The section was re-measured, this time driving to the right of the pothole, resulting in more consistent readings (current SI of 4.7 vs. new SI of 4.2).

In further investigating the physical characteristics of the profile it was noted that the wavelength of the pothole had a significant effect on two of the wavelength amplitudes. This is illustrated in Figure 2.4. The top half of this figure, illustrates

Figure 2.3 Pot Hole in Wheel Path of the Second 0.1 mile Section along Pearce Lane

subplots of the characteristics of the 0.1 mile section with the pothole, but driving to the left of the pothole, and the bottom half, illustrate three subplots of the 0.1 mile section immediately following the pothole section. Each set of subplots from left to right respectively, depict the differences between successive profile points, D_i', the power spectral components for the eight bands used in the new SI equation, P_i, and the profile, p_i. As can be noted from the figure, the two sets of three subplots of Figure 2.4 have similar characteristics.

Figure 2.5 depicts the same consecutive sections, except that the wheel path of the first section includes the pothole. As can be noted from Figure 2.5 the plots of D_i' and P_i are different. The spike shown in D_i' was found to be at the exact same location as the pothole, and the P'_i component of the wavelength of the pothole is much greater. Thus, the SI from the new wavelength is more affected by the pothole. The SI (and thus, IRI) of the current ride equation is not directly related to the wavelength component of the pothole and is thus, not as significantly affected.

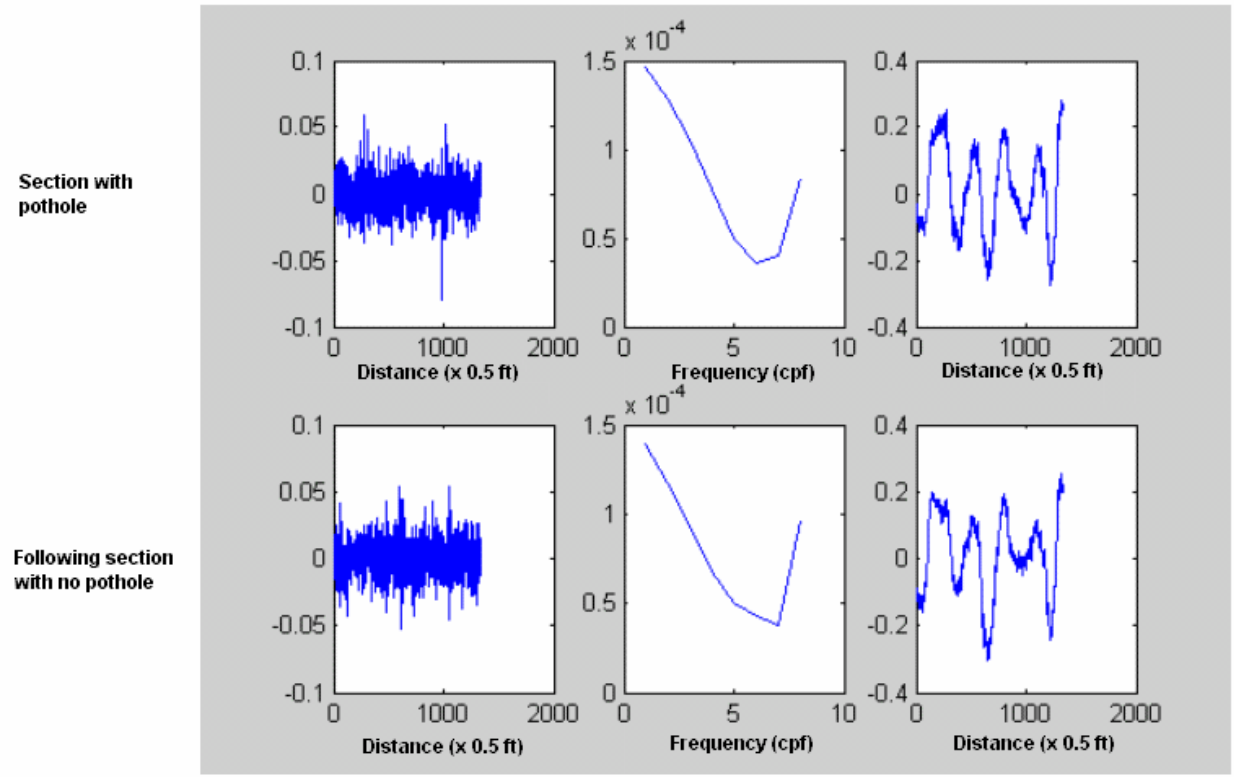

Figure 2.4 Two Successive 0.1 mile Pavement Sections – Pothole missed

From this example, it would appear as though the new ride equation is a better indicator of sections with localized roughness than the current SI equation, and thus IRI. One of the concerns on IRI, and hence the current SI model, is the averaging effect of the IRI statistic. The IRI statistic is based on the average of the predicted relative displacements between the sprung and unsprung masses of a quarter car model (Sayers, 1995). Whereas the effect of the pothole on IRI (and the current SI) over a short section would be more dramatic, its effect over the 0.1 mile or 528-ft distance was not as great. The pothole had a much greater effect on the SI computed from the new model. Additionally, the shape or weights placed on the frequencies of the IRI equation are fixed and the weights not selected based on a rating panel. Although the new SI model depends on the average amplitudes of the one to eight meter wavelengths, with eight statistics used to measure ride, it is more likely to better distinguish the pothole.

Because of the new equation's apparent capability to distinguish roughness features,

it was decided to investigate the use of the new model as a possible screening tool for finding bumps and dips. At the same time, the equation provides a prediction of what is acceptable to the rating panel in terms of ride. In the next section, we will investigate a method used for specifically locating the pothole and its characteristics, based on the correlation of a bump template with the road profile containing this

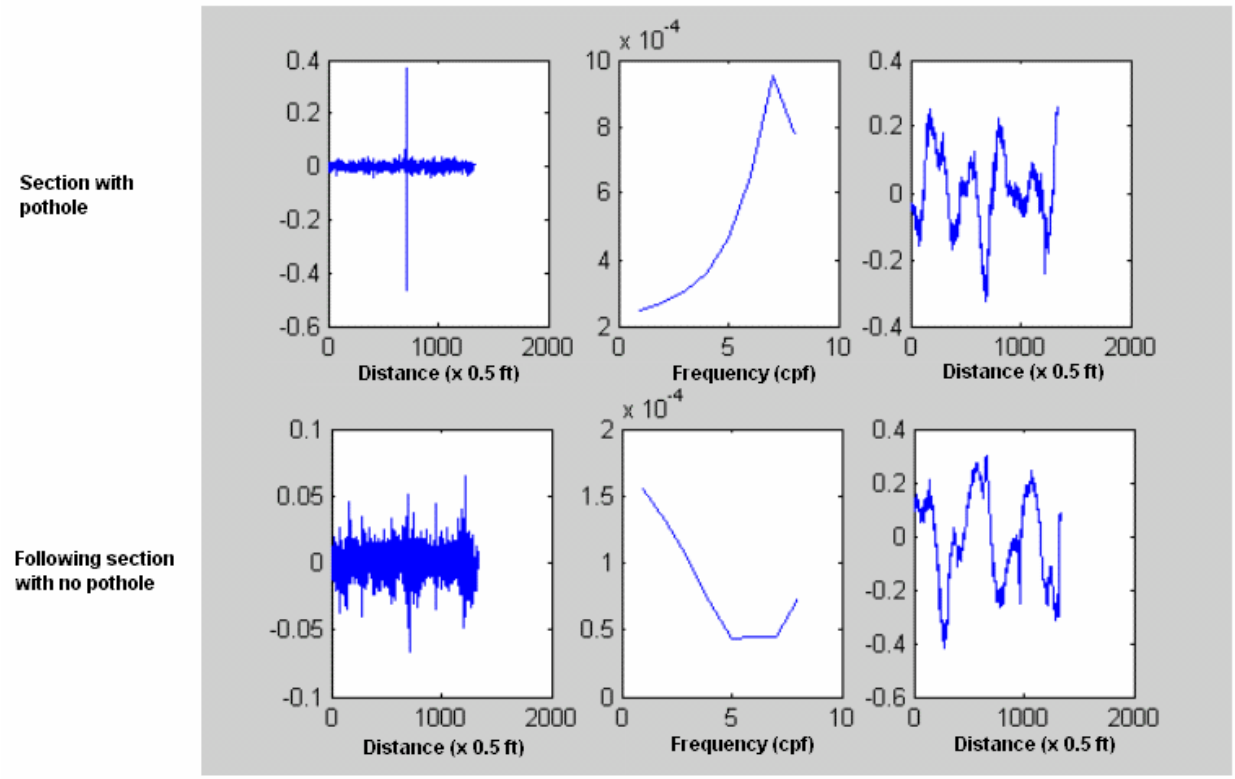

pothole.

Figure 2.5 Two Successive 0.1 Pavement Sections – Pothole in Wheel Path.

2.3 Cross Correlation Methods

During the mid 1980s, considerable problems existed in the use of the photocell detector on the Department's profiler for lining up repeat data measurements. Repeat runs were needed in order to better determine the repeatability of the profiler. Because of the frequent failure of the photocell detector, repeat measurements were often made using a small board placed under one of the wheel paths. The profile of this board was distinguishable by viewing the plots. The use of cross correlation of repeat runs easily found the position of the board with respect to each run pair. The two profiles were then lined up in accordance with this difference, and, because of the success of this method, a program was written at that time to automatically perform

this function.

Of course, more reliable and accurate detectors are now available on today's profilers. However, with the earlier successes, project researchers thought that the method might be useful for locating bumps and dips. Thus, cross correlation methods were investigated for finding the locations and magnitudes of bumps and dips. The cross correlation statistic is given in Equation 2.4 below.

$$r_{xy}(n) = \sum_{k=0}^{M-1} x(k)y(k+n), \quad 0 \le n \le M-1 \qquad (2.4)$$

The correlation function is often shown as the mean lagged product, or $E[x_k,y_{k+n}]$. Estimates of this can be obtained by dividing by N-n, depending on the definitions. The lineup procedures discussed above used equation 2.4 directly, and when the cross correlation between the two profile sets, x and y, was greatest, the number of lags was recorded and the appropriate set then shifted by this amount. Accounting for the end effects is one difficulty that must be addressed when cross-correlating finite length sequences. One method that can be applied is to assume that the profile of each section repeats or is periodic and use a circular method for cross correlation. This will be addressed further when discussing the template method.

For the methods in this report, equation 2.4 is used and the result then normalized in accordance with equation 2.5 so as to provide a unit-less number between plus and minus one.

$$\varphi_{xy}(n) = \frac{r_{xy}(n)}{\sqrt{r_{xx}(0) \times r_{yy}(0)}} \qquad (2.5)$$

For example, if a normalized cross correlation of two sets of sequences is performed, where one sequence is generated by a sine function, and the other, by a cosine function of equal amplitude and wavelength, the resulting sequence is a sine function shifted by 180° or π radians. The cross correlation between the two sequences is a maximum at 3π/2 or 270°, and a minimum at π/2 or 90°.

Ideally, uncorrelated or random data should not have any correlation. For a large finite number, N, of random numbers, it can be shown (Ifeachor and Jervis, 2002) that the variance of the values approach 1/N. A set of N, random data points generated by the Matlab function rand(), are illustrated in Figure 2.6. Figure 2.7 illustrates the autocorrelation for the data of Figure 2.6. Note that the value is a maximum of one for a zero lag, and then the values are distributed about zero. The cross correlation between the data of Figure 2.6 and a second similar set is shown in Figure 2.8. Also illustrated is the 95% confidence interval. That is, in 'the long run', about 95% of the points will fall within the illustrated range. In Figure 2.8, it is noted that at least three out of the 1000 data values exceed the 95% range.

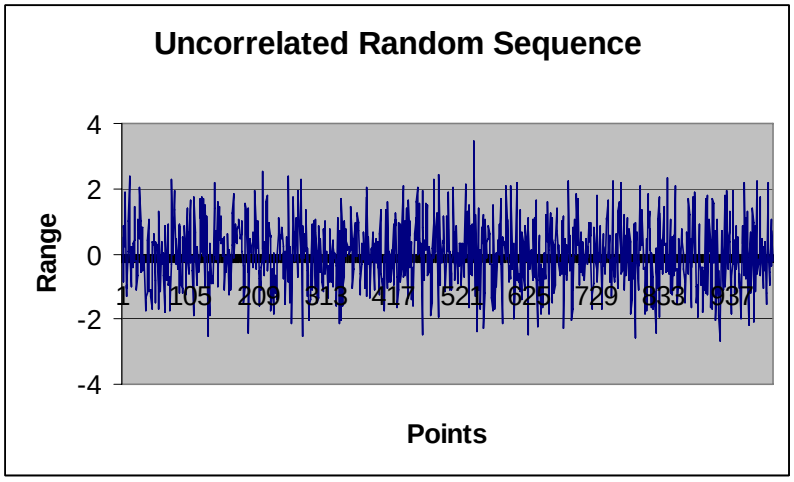

Figure 2.6 Random Data Sequence

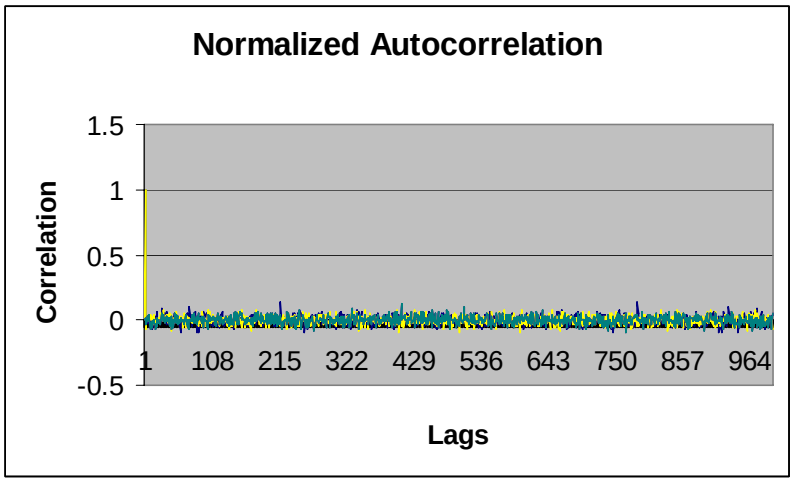

Figure 2.7 Autocorrelation of the Data in Figure 2.6

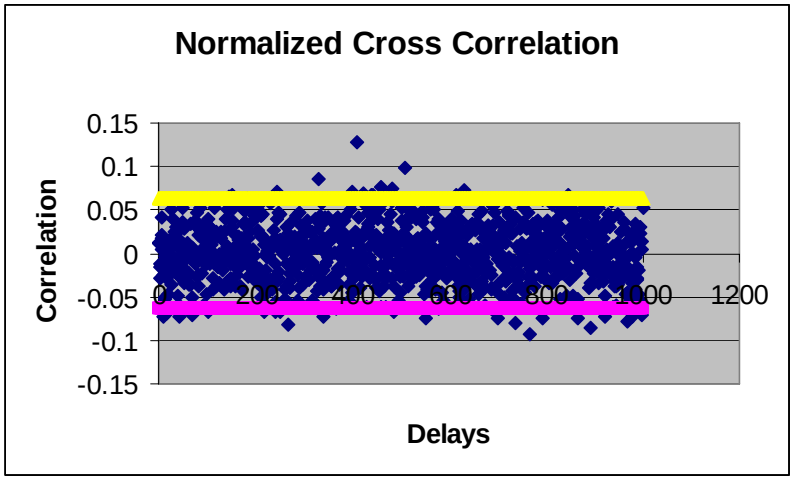

Figure 2.8 Cross Correlation of Two Data Random Sequences

From the above discussion, it would seem possible to use the cross correlation between a bump or dip with road profile as a possible means of identifying the magnitude and location of similar shapes in a pavement profile. Cross correlation used for this purpose is considered in the next section.

2.4 Cross Correlation for Finding Localized Roughness

In the previous section, it was shown how cross correlation can be used for making statistical statements about random or uncorrelated signals. In this section, cross

correlation will be investigated for identifying the location of the pothole noted earlier. The cross correlation between the profile of the section with the pothole and an appropriate bump signature should give a larger magnitude when the bump signature is shifted over the pothole than when it is not covering the pothole. Thus, researchers decided to determine a typical bump signature that could be investigated for cross correlation with the pothole profile found in the Pearce lane section to determine if this method could identify the location of the pothole.

The artificial bumps developed by previous research at TTI as discussed in Chapter 1 (Table 1.1) were investigated to determine if one of these could be used for the cross correlation. Each bump was profiled and inserted into various smooth profiles. A spline function was used for joining the ends of each bump into the middle of each profile. Although any of the bumps would have worked, bump 5 of Table 1.1 was selected as the 'typical' bump or bump signature as it seemed to consistently have one of the smoother transitions when inserting the bump into various profiles for study. Figure 2.9 depicts bump 5 located on one of the test sections at the Texas A&M Riverside Campus. Figure 2.10 provides a profile of this bump.

Figure 2.9 Photo of Bump 5 on Pavement Test Section

This bump was then cross correlated with the profile from the section on Pearce Lane that included the pothole. Figure 2.11 illustrates the cross correlation results. The sharp peak illustrated in the cross correlation results depicts the location of the bump. With each point representing approximately 0.5 feet, the location of the peak was found to be at the exact location of the pothole.

From the results discussed in this chapter, two important conclusions can be made. First is that the new SI (NSI) from the new equation is more sensitive to the presence of localized roughness over a 0.1-mile section than either IRI or the current SI, at least on the Pearce Lane section. The second one is that the cross correlation method, using the profile of an artificial bump, was able to physically locate the pothole within the Pearce Lane section. In the following chapter, the effects of adding artificial bumps in the profile on IRI and NSI are investigated. Then, a general bump template procedure for identifying areas of localized roughness is proposed.

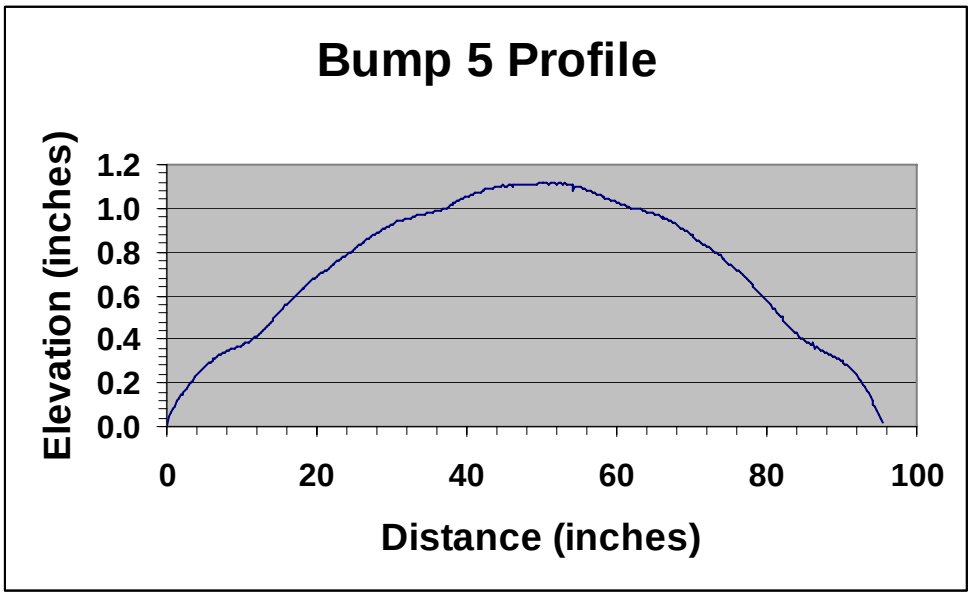

Figure 2.10 Bump 5 Profile.

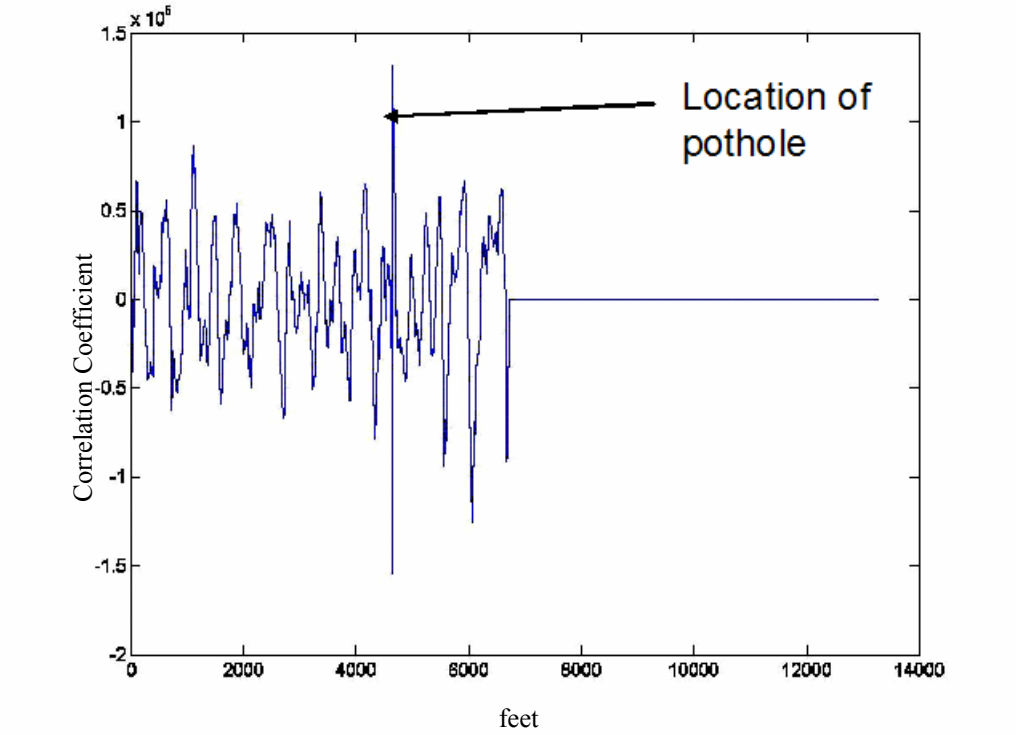

Figure 2.11 Cross Correlation Results.

Chapter 3
Localized Roughness Identification Methods

3.1 The Effect of Simulated Bumps on IRI and NSI

In the previous chapter it was noted that the new SI equation was better able to locate a pothole, in the profile on one of the Austin Test Sections than either the current ride equation or IRI. In this chapter, a procedure is introduced for cross correlating a bump template with various road profiles to locate areas of localized roughness, i.e., bumps and dips. Beforehand, however, we will investigate the effect of bumps with different lengths and amplitudes on the IRI and ride statistics.

For investigating the effects of the simulated bumps, a set of profiles with bumps and dips were generated by changing the amplitude and length of bump 5 and inserting this bump into a smooth profile from Pearce Lane. The first set of profiles were generated by inserting each bump into the Pearce Lane profile, changing the amplitude of bump 5 to 0.125, 0.25, 0.5, 0.75, 1.0 and 2.0 times its original height of 1.116 inches, or 140, 279, 558, 837, 1116, and 2232 mils. In a similar manner, a second set of bumps were made, this time holding the original amplitude constant and varying the lengths to two, three, and four times the original length of eight feet, resulting in a set of 1116-mil bumps of 8, 16, 24, and 32 feet in length. The process was repeated to generate dips by reversing the amplitudes. The bumps are illustrated in Figures 3.1 and 3.2. The dips are illustrated in Figures 3.1 and 3.3. For each profile generated, the current SI, the IRI, and new SI were computed. The SI, IRI, and NSI statistics for the various combinations are illustrated in Tables 3.1 to 3.3.

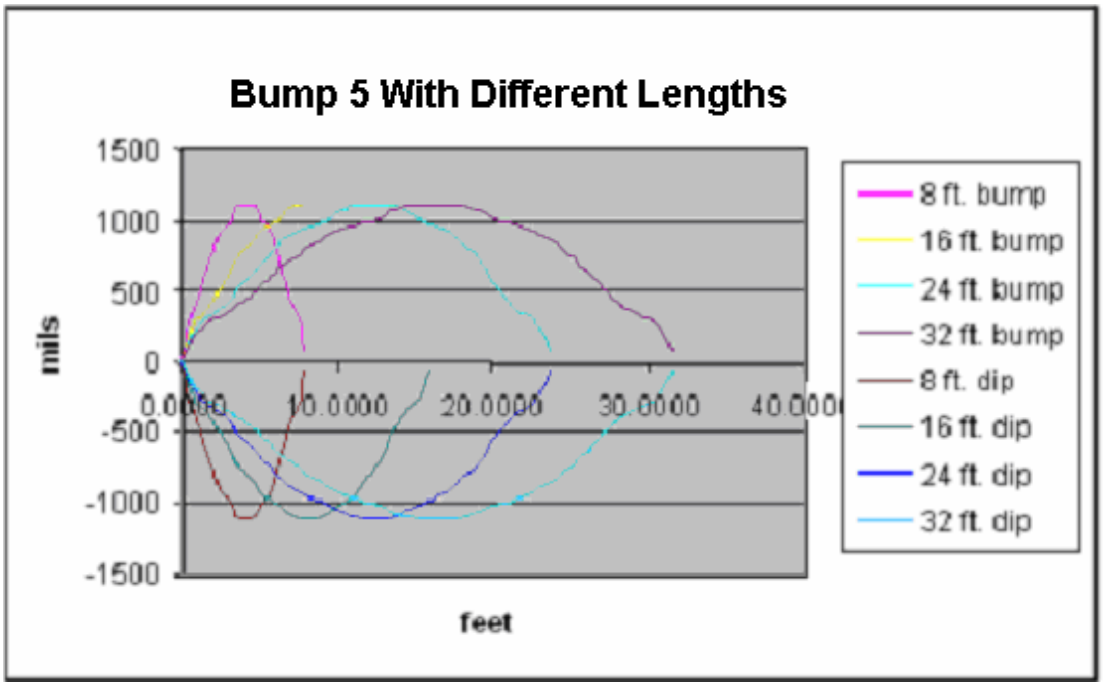

Figure 3.1 Bump 5 with Varying Lengths

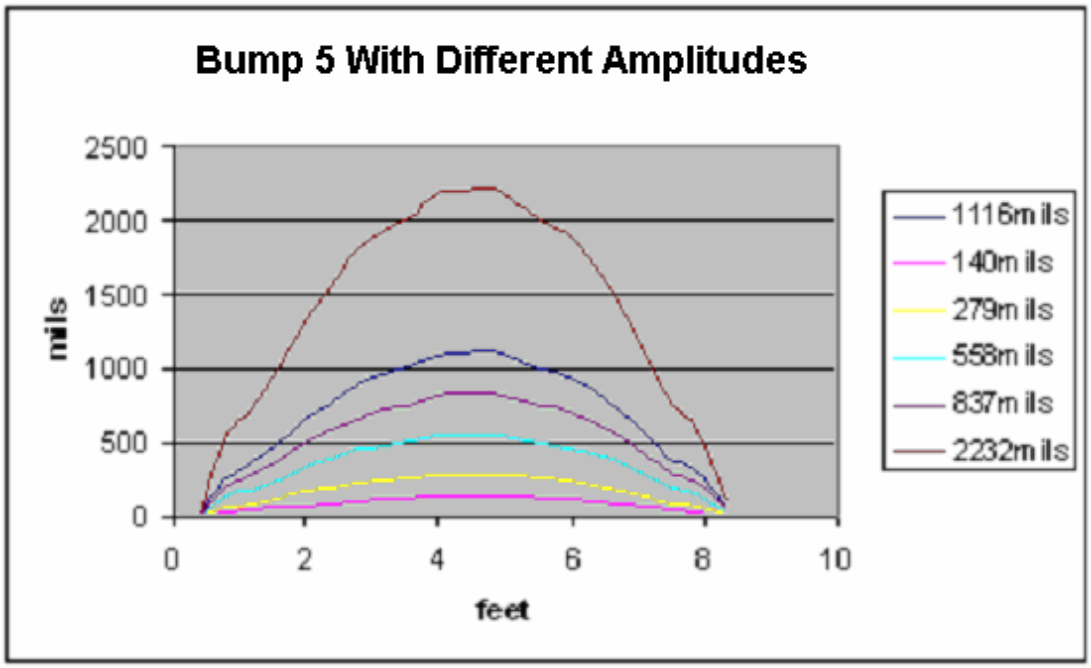

Figure 3.2 Bump 5 with Varying Amplitudes

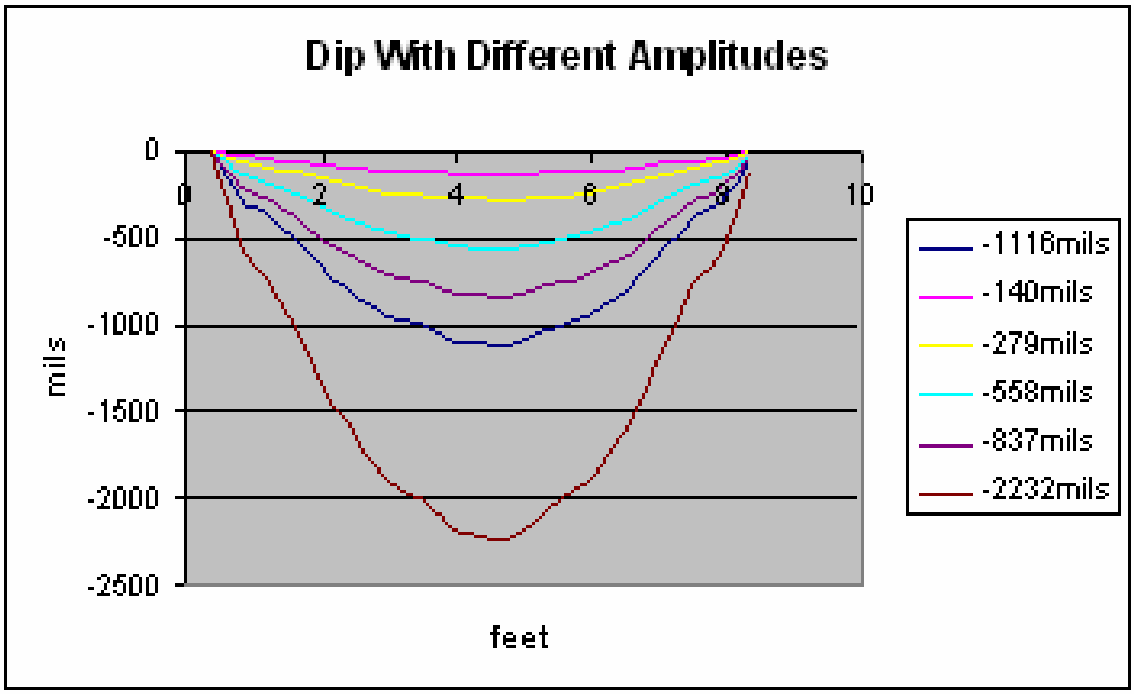

Figure 3.3 Reversing Bump 5 for Generating Dips

Table 3.1 NSI Values for Different Amplitudes and Lengths

NSI	amplitude (mils)					
length (feet)	140	279	558	837	1116	2232
8	3.67	3.37	2.78	2.29	1.87	0.83
16	3.92	3.73	3.32	2.92	2.57	1.50
24	4.22	4.06	3.72	3.40	3.10	2.13
32	4.60	4.57	4.26	3.91	3.49	2.62

Table 3.2 SI Values for Different Amplitudes and Lengths

SI	amplitude (mils)					
length (feet)	140	279	558	837	1116	2232
8	4.4	4.3	4.1	3.9	3.7	3.1
16	4.4	4.3	4.1	3.9	3.7	3.0
24	4.5	4.4	4.1	3.9	3.8	3.0
32	4.5	4.4	4.2	4.0	3.8	3.1

Table 3.3 IRI Values for Different Amplitudes and Lengths

IRI	amplitude (mils)					
length (feet)	140	279	558	837	1116	2232
8	1.01	1.08	1.21	1.36	1.52	2.17
16	1.01	1.07	1.22	1.38	1.54	2.20
24	0.97	1.04	1.19	1.36	1.53	2.21
32	0.93	1.00	1.15	1.31	1.45	2.12

The values in Tables 3.1-3.3 and corresponding plots in Figures 3.4-3.8 illustrate the effect of the amplitude and wavelength variations on SI, IRI, and NSI. In particular, note in Figure 3.4 that IRI (and thus SI) changes with bump amplitude, but very little by bump wavelengths, (Figures 3.6 and 3.7). On the other hand, NSI changes with both amplitude and length, as may be observed in Figures 3.5 and 3.8. From these results, it can be concluded that the new SI equation seems much better at distinguishing length variations for the range indicated than IRI or the current SI.

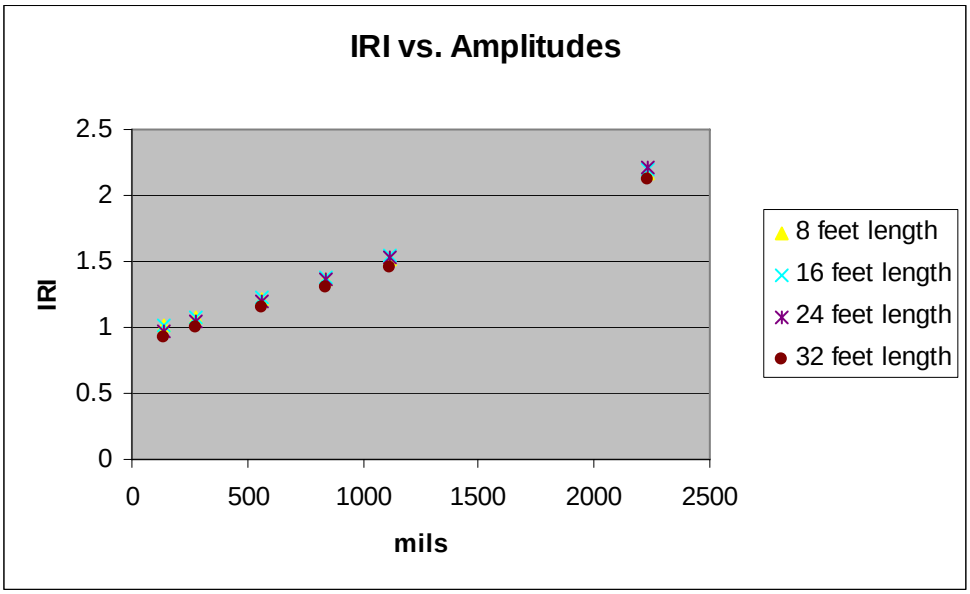

Figure 3.4 IRIs of Artificial Bump Profiles with Varying Amplitudes

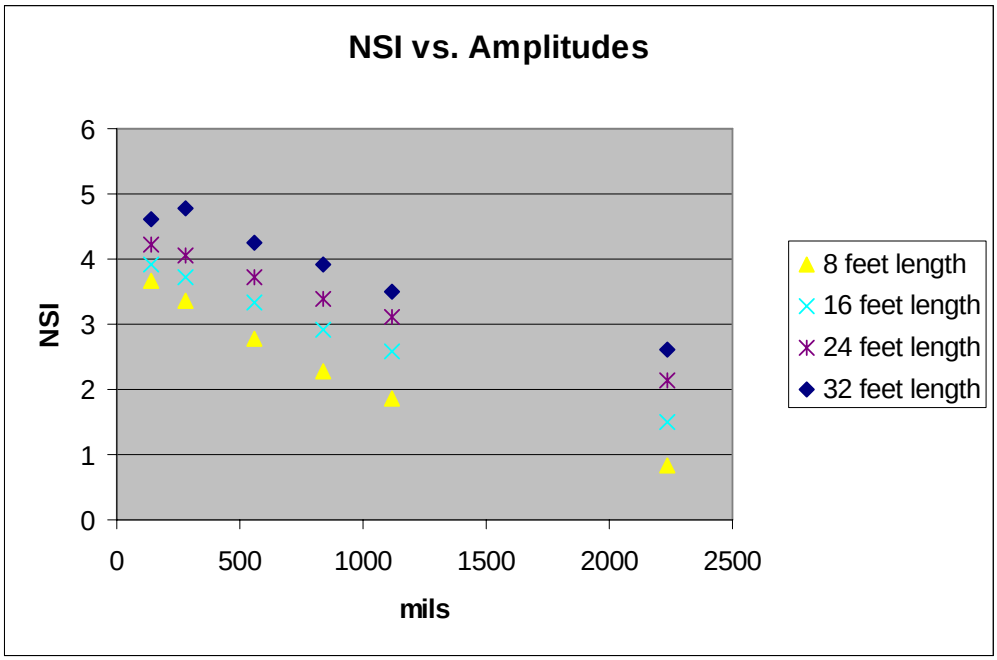

Figure 3.5 NSIs of Artificial Bump Profiles with Varying Amplitudes

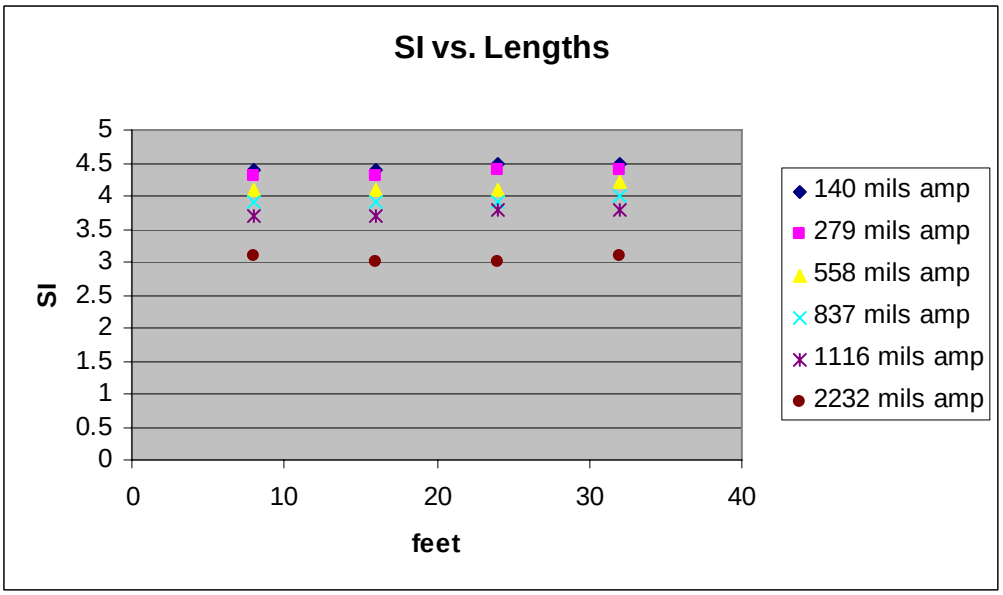

Figure 3.6 SIs of Artificial Bump Profiles with Varying Lengths

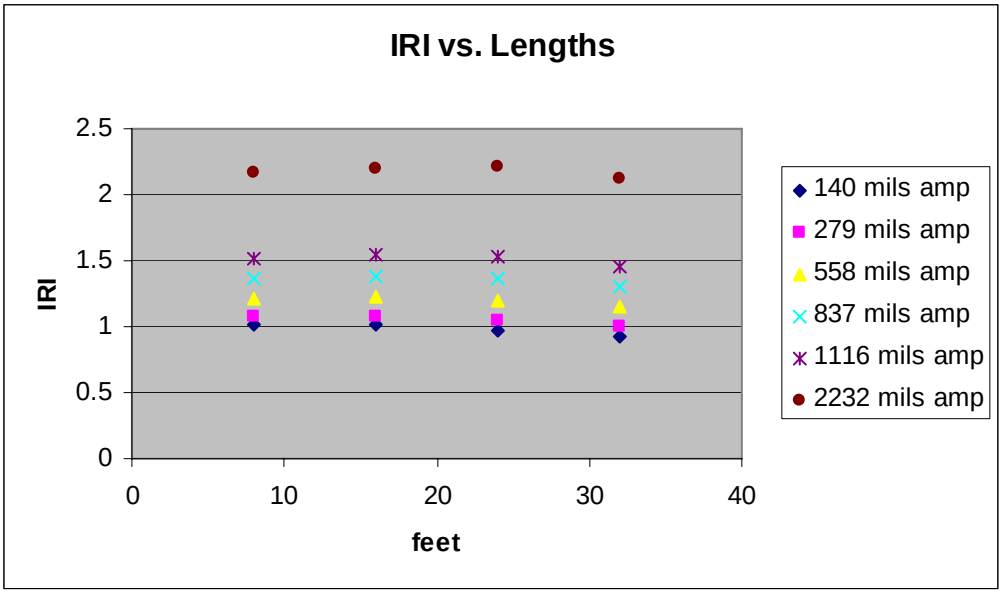

Figure 3.7 IRIs of Artificial Bump Profiles with Varying Lengths

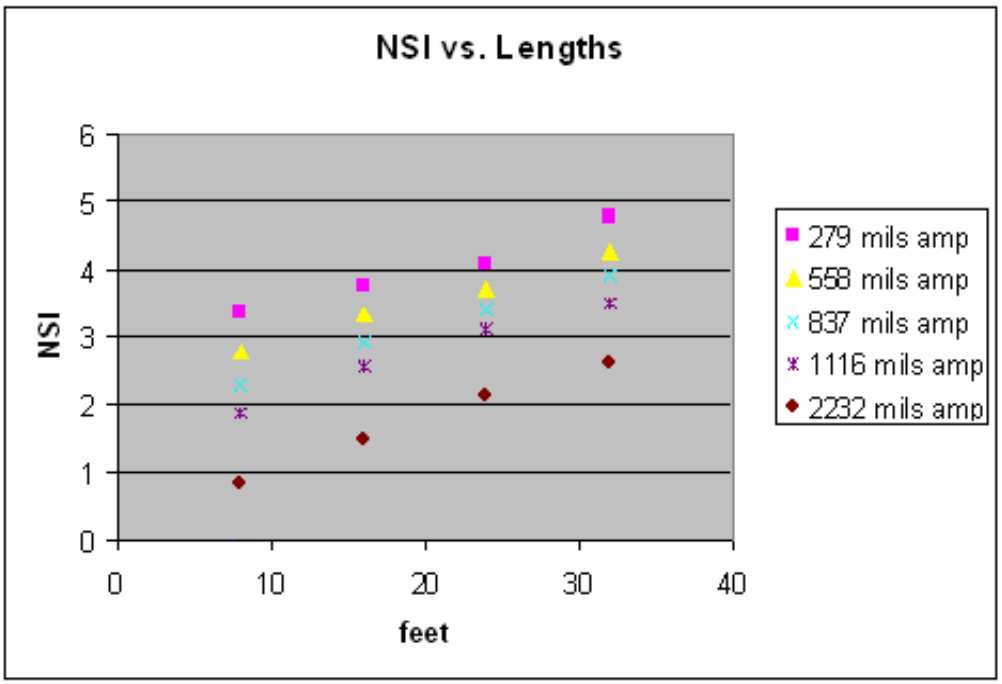

Figure 3.8 NSIs of Artificial Bump Profiles with Varying Lengths

As noted in the last chapter, the autocorrelation of the section with the pothole on Pearce Lane resulted in identifying the exact location of the pothole. In the next section, we will investigate the cross correlation of the various versions of bump 5

with the measured profile of a road section with bump 5 actually on the section.

3.2 Cross-Correlation of Bump 5 Templates with a Measured Bump 5 Profile

Bump 5 was placed on a pavement section at the Texas A&M Riverside Campus and the profile was measured with a TxDOT profiler. The various lengths of the bump 5 templates described in the previous section were then cross correlated with the profile of the section where bump 5 is physically placed on one of the wheel paths. By cross correlating the measured profile with bump templates of varying lengths, we would expect that the template with the correct length and amplitude will correlate best with the profile. This turned out to be the case as illustrated in Figure 3.9. The peak illustrated in the plot with the cross correlation results indicated the exact location of bump 5 on the test section. The template that correlated best with the bump was the bump 5 template.

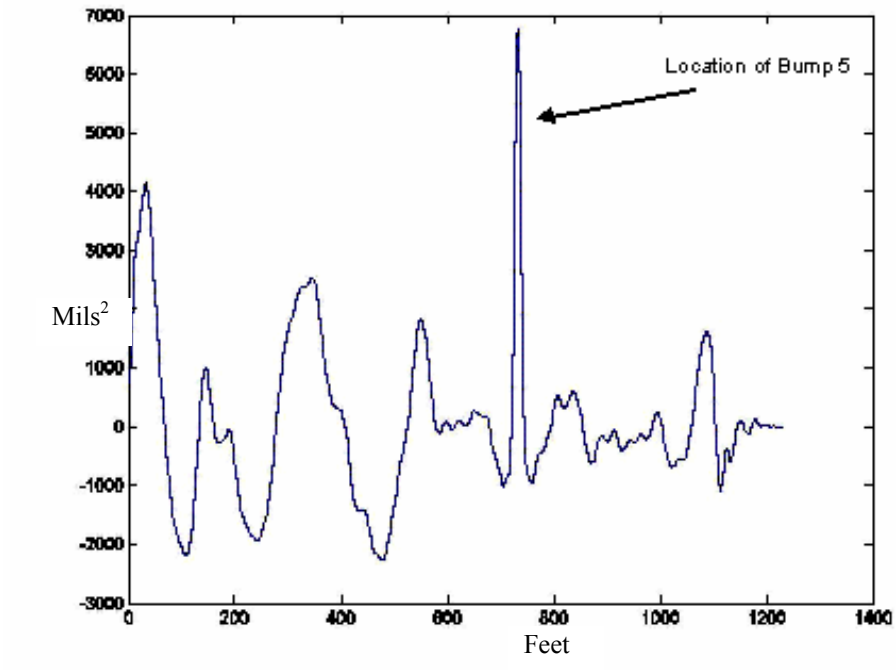

Figure 3.9 Cross-Correlation of Bump 5 in 0.2-mile Test Section

With the results of the cross-correlation method using the bump 5 templates, it was proposed to use a similar process as a general means of locating bumps and dips in profiles of various pavements. In the next section, a procedure is described using the process of cross correlation of bump templates with measured pavement profiles for

evaluating localized roughness.

3.3 Template Analysis Procedure (TAP)

Based on the results noted in the previous sections on using cross correlations with the new SI equation, the following procedure for detecting defects is proposed:
The TAP Procedure consists of two parts: a. Establishing the TAP thresholds, and b., using the thresholds to identify localized roughness.

> **Establishing the Threshold:** A set of NSI levels are first identified that are considered acceptable for each road type (Farm to Market, Interstate Highway, etc). Then for each level the set of roads with NSI values equal to or greater than the selected NSI are found and their respective cross-correlation values with the six predefined bumps lengths computed. The maximum correlation for each road is found and averaged with the other maximum correlations in the set. This average is then used to compute the threshold. Thus there will be a threshold determined for each NSI level and each bump length of interest. Ideally, finding the appropriate thresholds should only be necessary one time. After that, all future applications would use this set.
>
> **To Identify Areas of Localized Roughness:** A desired NSI level for the road section to be tested is determined. The NSI is determined for each section. If the NSI is equal to or greater than the desired NSI reading, the sections needs no further action. If this is not the case, the cross-correlation procedure is applied and the areas of localized roughness are identified.

For example, suppose the set of thresholds have been identified for the NSI value of 4.0 and it is desired to test a specific pavement section. The profile is first obtained and then read into the TAP program. If all NSI levels are greater than 4.0, the road section is ok. If one or more subsections of the pavement are below the desired NSI, the particular bump and dip locations and magnitudes are identified and printed.
This selection procedure is illustrated in Figure 3.10. The profile of each 0.1 mile section is cross correlated with variations of bump 5. The amplitude is fixed at one-

inch and bumps are generated for wavelengths of four, eight, twelve, sixteen, twenty, and twenty-four feet. Dips will not be generated as the correlation values for dips matching the same lengths as bumps will simply have negative readings. The first derivative of each newly generated bump (Figure 3.11) for each of the six wavelengths are systematically cross-correlated with the first derivative of the section profile being investigated, yielding a set of correlation values that indicates how closely a particular area in the section follows the different bump templates. The absolute value of the correlation statistic is then compared to a threshold. If one is found to exceed this correlation threshold level, a bump (or dip if the original correlation is negative) is recorded. The magnitude of the bump or dip can then be determined from the profile of the section at the located point. Note that the amplitude of the bump template is not necessarily the amplitude of the physical bump. Initially, researchers thought of varying the amplitude of the bump template in addition to its wavelength. However, in practice, once a bump is located, one would have to examine the profile at that location anyway to determine the actual shape of the bump. A newer version of the procedure has incorporated a method for estimates of amplitude.

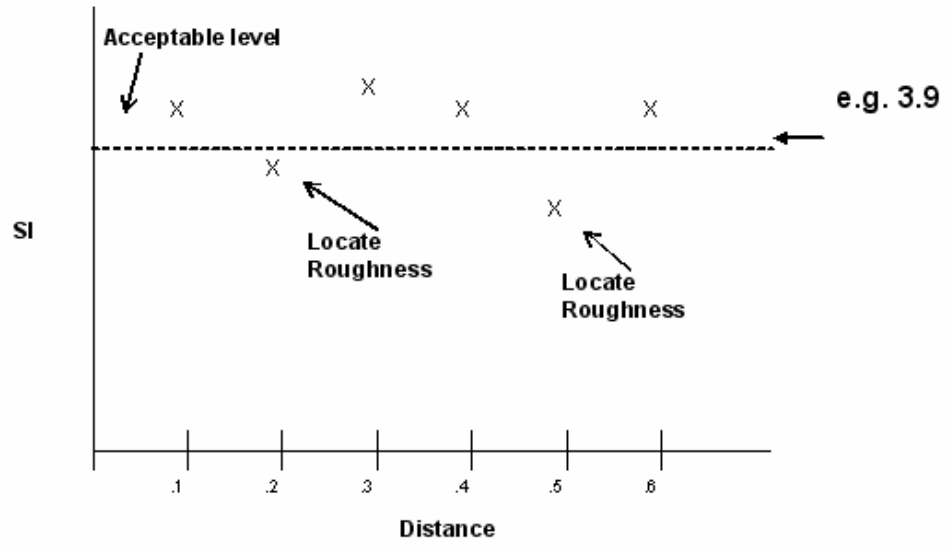

Figure 3.10 Identification of Areas for Cross Correlation Analysis

3.4 Additional Comments on Selection of the Thresholds

The threshold level is important to proper bump identification. For example, in order to select an appropriate threshold level, a set of pavements with NSIs at or above the desired NSI level are identified. That is, the pavement engineer selects a desired NSI level. An unbiased sample of 0.1 mile pavement sections where the NSI levels are at or above the desired level is then selected and the profiles are cross correlated with the set of six bumps, recording the maximum correlation. The NSI values from Project 4901 data were used for computing the initial threshold values.

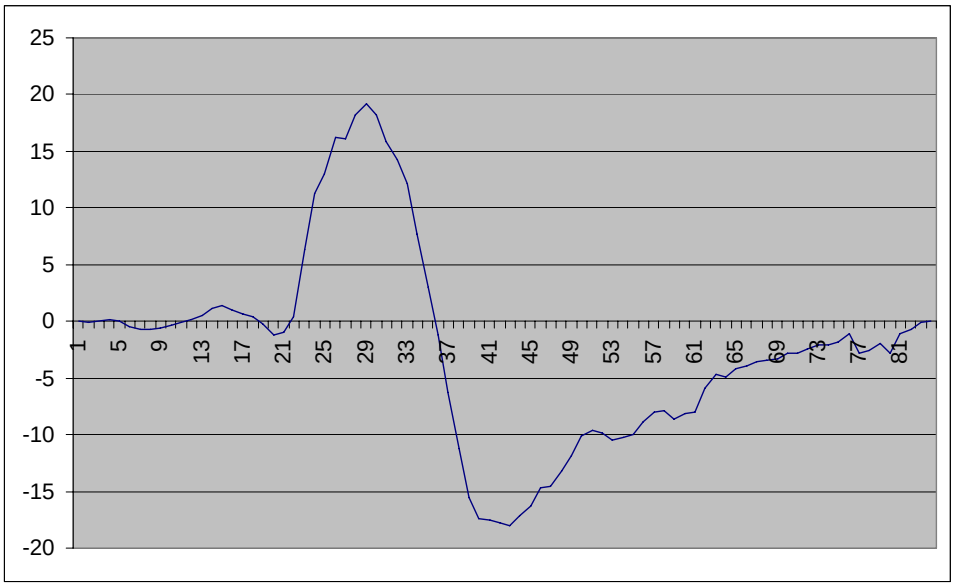

Figure 3.11 First Derivative of Bump 5

Each of these maxima is used to estimate the mean of the maximum correlation value expected from pavements with the chosen NSI level. The estimate of the sample variance of the means is used for computing a confidence level for the maximum acceptable correlation value. The correlation threshold for evaluating localized roughness at a given confidence level is then defined in equation 3.1 below:

$$T_{nsi} = r_{max} + Z^* \frac{\sigma}{\sqrt{n}} \qquad (3.1)$$

Where T_{nsi} = maximum desired correlation threshold

r_{max} = mean of the sample of maximum correlation values for a given acceptable NSI

Z = the desired normal or t distribution confidence area

n = sample size

σ = the unbiased estimate of the population standard error.

In the following chapter, the Template Analysis Procedure is applied to a set of pavements from a construction project performed along US 290 near Brenham during 2003.

Chapter 4
Application of Template Analysis Procedure

In this chapter, the template analysis procedure is applied to field data collected on a rehabilitation project. The intent is to identify a suitable project where the surface profiles can be measured before and after repairs to establish the locations of defects using the template analysis procedure. The location of defects can then be compared with those identified using SS 5880.

4.1 Rehabilitation Project

Researchers identified a suitable project along US 290 in the Bryan District where the existing asphalt concrete pavement was resurfaced. This project began at the junction of US 290 and SH 36 in Brenham and proceeded westward for about 12 miles. Further details of this project are included in Appendix A. The project was let under the straightedge specification, and had numerous defects along its length as determined from the straightedge.

The Bryan District provided surface profile measurements taken on the travel lanes before the contractor undertook repairs on the project. After repairs, surface profiles were again measured using an inertial profiler from the Materials and Pavements Section of TxDOT's Construction Division. The contractor ground out the bumps at the locations determined from the straightedge. Researchers established the locations where the contractor undertook repairs along the US290 project to take out defects identified by the engineer and the contractor using the straightedge. Table A10 in the appendix summarizes the locations of these corrections.

As discussed, in Chapter 3, the template procedure involves the cross-correlations of bump templates with the pavement profiles. The four west- and east-bound lanes, L1, L2, R1 and R2, were selected for the investigation and the template procedure applied to the profile data collected on these lanes. Figures 4.1 and 4.2 provide profile plots of the L1A, L2A, R1A and R2A profiles before repairs were made. Figures 4.3 and 4.4 provide plots of the L1B, L2B, R1B and R2B profiles after repairs.

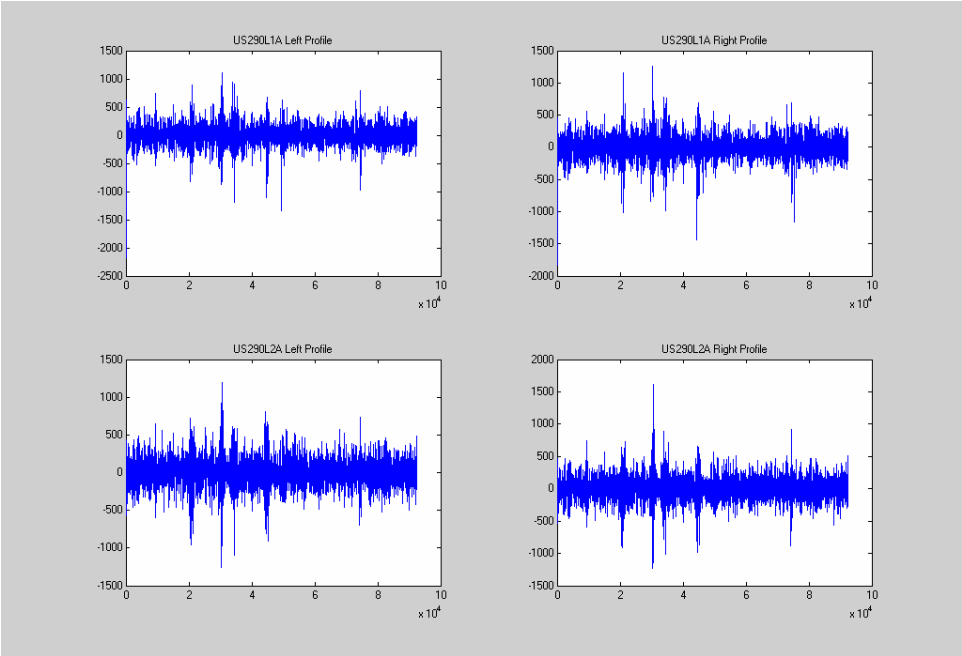

Figure 4.1 US290 L1A and L2A Profiles before Repairs

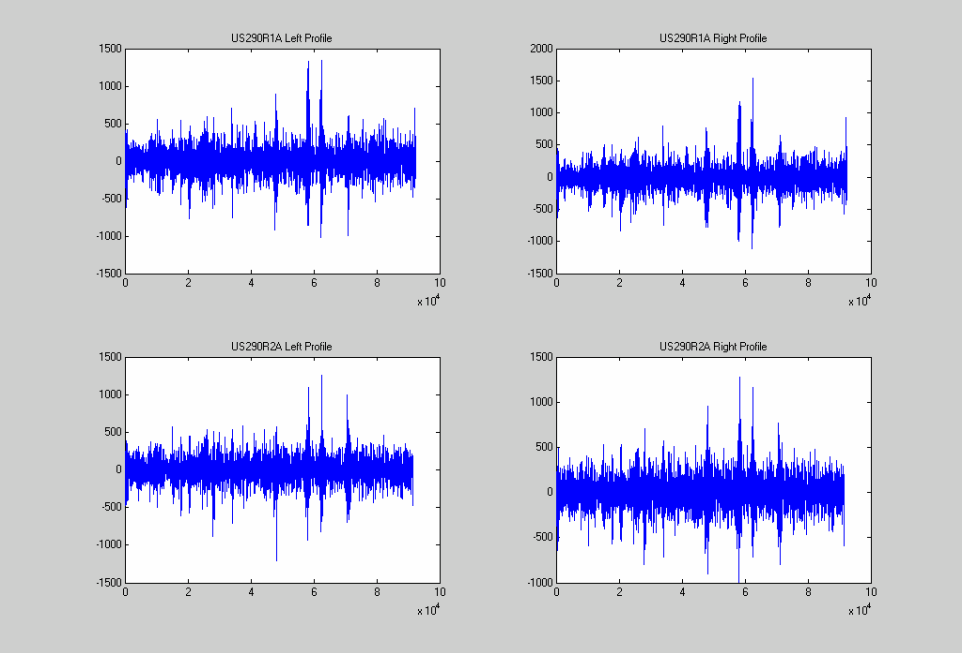

Figure 4.2 US290 R1A and R2A Profiles before Repairs

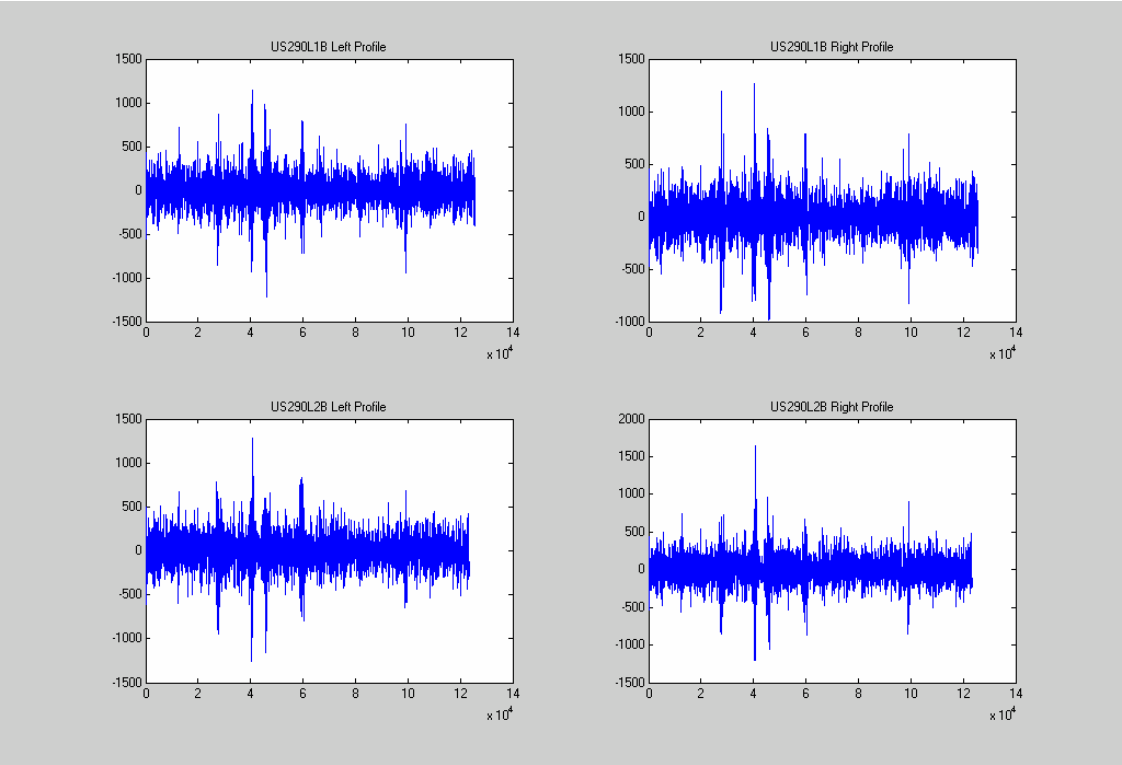

Figure 4.3 US290 L1B and L2B Profiles after Repairs

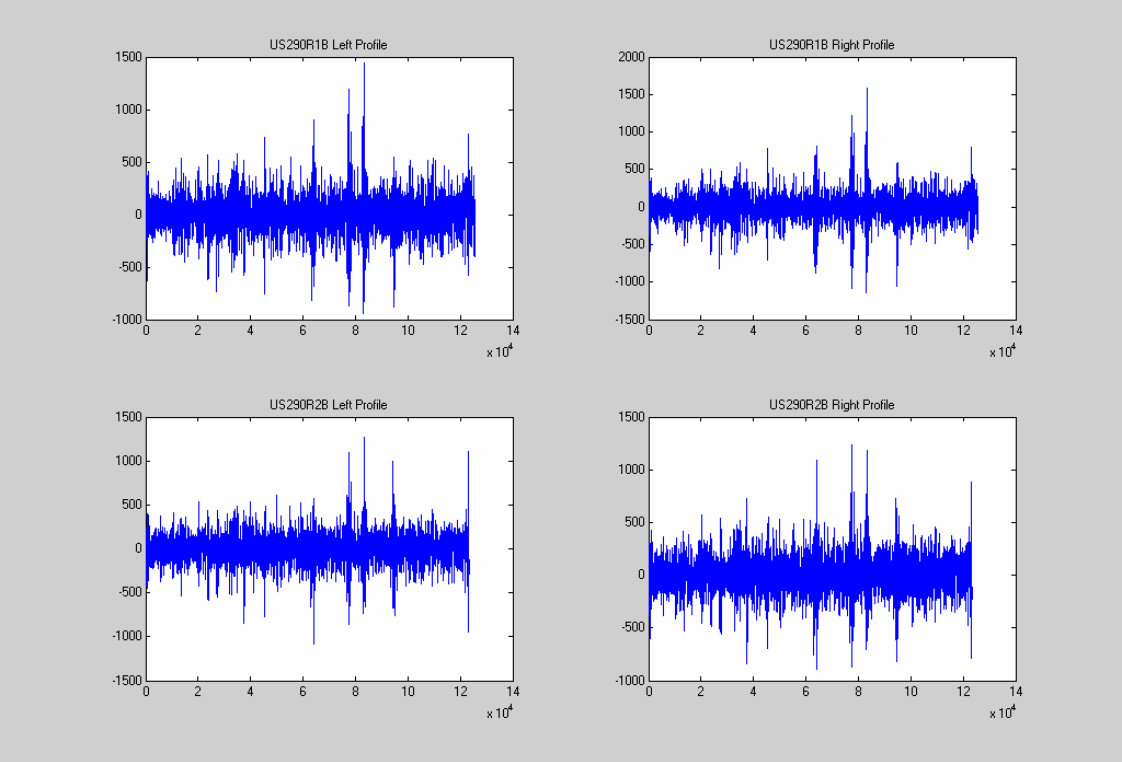

Figure 4.4 US290 R1B and R2B Profiles After Repairs

4.2 Computer Program Used for Template Analysis Procedure

As previously discussed, a program written in Matlab was developed to implement the template analysis method. The analysis program, after reading the profile of the pavement section of interest, first determines the number of one mile sections in the profile. The program then performs a cross correlation between the profile for each one mile section with the appropriate bump template. As noted in previous chapters, the template is derived from the artificial bump 5. A cubic spline function is used to generate the 4-, 12-, 16-, 20- and 24-foot templates of the same general shape as the eight-foot bump. After the program finishes running the correlation, it then examines the PSI values and denotes or outputs those locations where the correlation values exceed a specified threshold. The analysis flow chart of this Matlab code is provided in Figure 4.5 below.

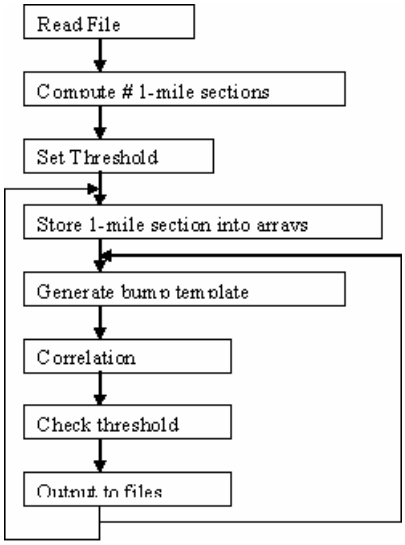

Figure 4.5 Template Analysis Program Flow

As discussed in Chapter 3, the standard error of the maximum correlation value for a group of sections with an acceptable NSI is used to compute the confidence interval for bump or dip identification as specified by equation 3.1. The threshold value used for distinguishing each bump is treated as a statistic that represents the percent confidence assigned for detecting bumps or dips. Confidence intervals corresponding to the 95%, 97%, 99%, and 99.99% significance levels were computed resulting in the threshold values 0.067130, 0.074322, 0.079631, and 0.088193 respectively.

Two functions are integrated into the Matlab code. The first is to count the total number of bumps/dips that the program detects in each one-mile section and throughout the profile data. The second computes the power-spectrum density value of the profile.

4.3 Results from the Template Analysis Procedure

The results of applying the Template Analysis Procedure on the L1, L2, R1, and R2 surface profiles are illustrated in Tables 4.1. This table compares the total number of bumps and dips found using the TAP and SS5880. As may be observed, the proposed TAP method finds more bumps than the current methods, SS5880 and Item 585.

Differences can be expected because of the two unrelated procedures used by SS5880/Item 585 and TAP for bump/dip identifications. Another difference could be because of the counting method used by TAP. TAP provides a count of all bumps and dips found for each template length interval. Some will overlap with one another, i.e., a bump (dip) can be a part of another, of different

Table 4.1 Bumps/Dips Identified

Table 4.1a

SECTION	SS5880	TAP
L1A	15	10
L2A	33	25
R1A	9	10
R2A	20	13
L1B	12	25
L2B	23	55
R1B	7	15
R2B	24	39

Table 4.1b

SECTION	Item 585	TAP
L1A	15	10
L2A	32	25
R1A	6	10
R2A	17	13
L1B	11	25
L2B	21	55
R1B	7	15
R2B	21	39

width, or it could be contained entirely within another bump of longer width. These two cases are illustrated in Figures 4.6 and 4.7. If the bump overlaps a second, then the repair area should include the largest area covering both bumps. If a set of overlapping bumps is counted as one, the number of defects determined using TAP is reduced as illustrated in Table 4.2.

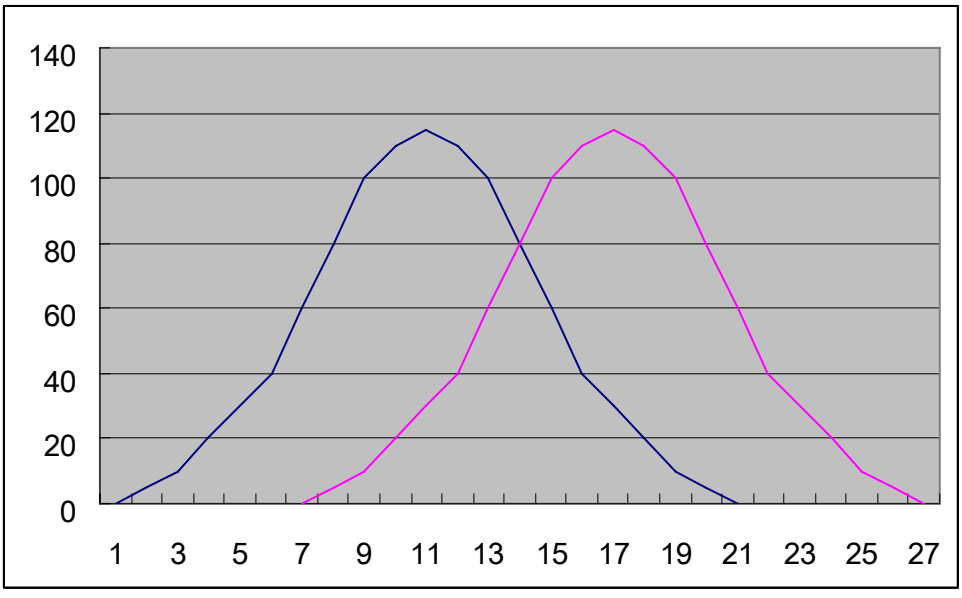

Figure 4.6 Example of Overlapping Bumps

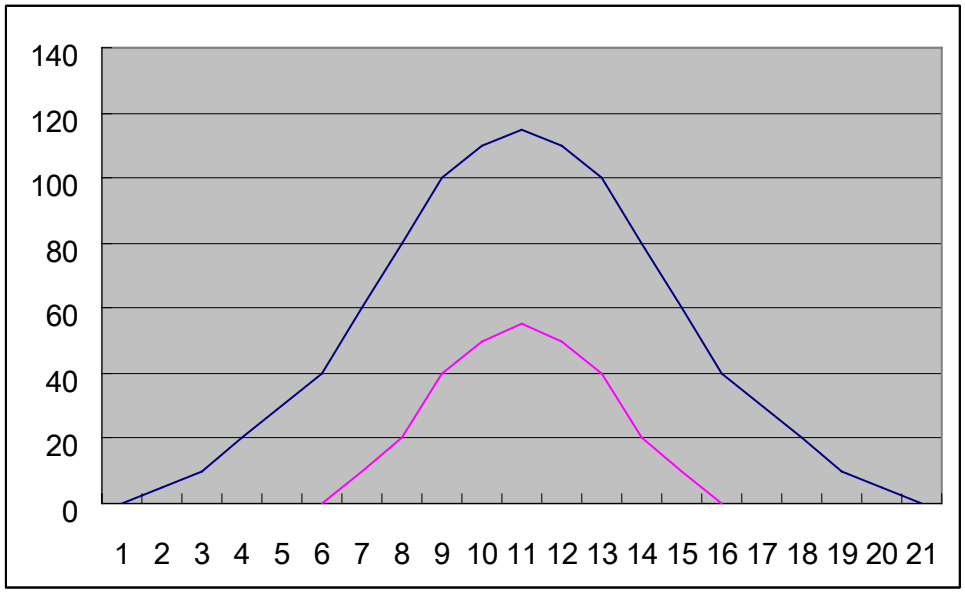

Figure 4.7 Example of a Bump Contained Within Another

Table 4.2 The Number of Bumps (Dips) Found Using The Corrective Procedure

Table 4.2a

SECTION	SS5880	TAP
L1A	15	3
L2A	33	7
R1A	9	5
R2A	20	5
L1B	12	7
L2B	23	12
R1B	7	6
R2B	24	10

Table 4.2b

SECTION	Item 585	TAP
L1A	15	3
L2A	32	7
R1A	6	5
R2A	17	5
L1B	11	7
L2B	21	12
R1B	7	6
R2B	21	10

The program first implements the template procedure, listing all bumps or dips found for each length and confidence limit combination. A second program then adjusts the list for overlapping bumps.

As discussed, the search for bumps using the method is a function of the NSI value selected for each 0.1-mile section. The following eight tables illustrate how the number of bumps or dips found varies with NSI. The first four tables, 4.3 to 4.6,

consider all bumps and dips. The next four tables, 4.7 to 4.10, only include the non-overlapping cases. Tables 4.3 and 4.7 show how the number of bumps or dips changes based on the selected NSI before repair. Tables 4.4 and 4.8 list the numbers after repair. The tables indicate the importance placed on the NSI selection criteria.

Tables 4.5, 4.6, 4.9 and 4.10 are similar to Tables 4.3, 4.4, 4.7 and 4.8, respectively, but compare the total bumps found by SS 5880 and template methods as a function of the NSI levels before and after repair. In Tables 4.5, 4.6, 4.9 and 4.10, the number found by the current method is denoted by the letter C, and the new method by the letter N. The three columns for C=N, C>N, and C<N provide the counts of the numbers of areas found equal or different between the two methods. Note that the total number of defects detected using SS 5880 does not vary with the selected NSI level. This total for a given lane is determined by adding the number of occurrences for C=N and C>N as illustrated in Figure 4.8. It might also be noted that the small amount of grinding done on some of the sections made only marginal improvements on SI and in some cases worst ride reported by NSI. This could be due to the fact that NSI is related to ride, whereas SI is related to IRI and the ride actually got rougher.

Or it could be because of other factors, such as the computation procedures, etc. Additional tests would be needed to evaluate this case.

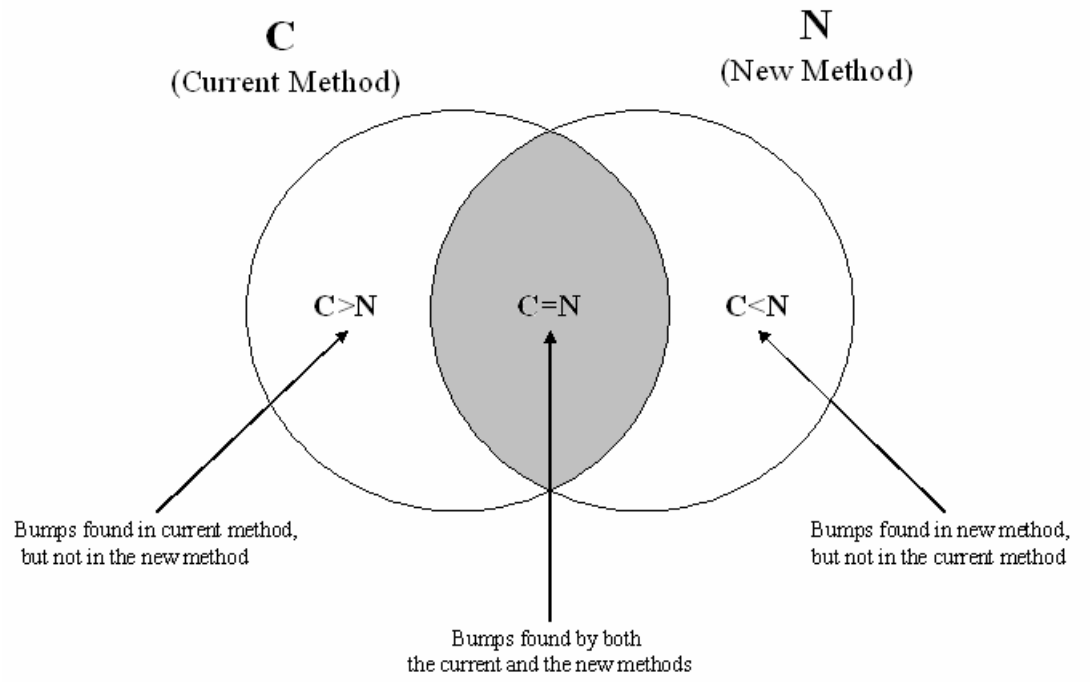

Figure 4.8 Relationship of Proportional Bumps Found by the Current Method and the New Method

From the tables, it is noted that, for most cases, the closest NSI level to where C>N and C<N lines cross is from 3.73 to 3.75.

Table 4.3 Number of Bumps for each 0.1 mile Section before Correction US290 (All)

	Lane			
PSI	L1A	L2A	R1A	R2A
3.60	3	8	2	4
3.61	3	8	3	4
3.62	3	10	3	5
3.63	4	13	3	6
3.64	4	16	3	6
3.65	4	16	3	6
3.66	4	18	3	8
3.67	6	18	4	8
3.68	7	18	4	8
3.69	7	18	6	9
3.70	8	20	7	10
3.71	8	22	7	12
3.72	9	25	8	13
3.73	10	25	10	13
3.74	12	29	10	15
3.75	15	33	10	16
3.76	17	35	11	17
3.77	18	38	12	17
3.78	18	40	12	17
3.79	21	42	13	18
3.80	21	44	13	18
3.81	23	45	14	19
3.82	26	46	14	20
3.83	26	47	14	22
3.84	26	49	14	23
3.85	27	52	14	25
3.86	27	52	15	26
3.87	27	53	20	28
3.88	28	53	21	31
3.89	31	54	21	33
3.90	32	55	22	34

Table 4.4 Number of Bumps for each 0.1 mile Section after Correction US290 (All)

	Lane			
PSI	L1B	L2B	R1B	R2B
3.60	9	32	5	20
3.61	9	33	7	20
3.62	9	35	7	22
3.63	12	36	7	23
3.64	13	40	8	24
3.65	13	44	8	26
3.66	15	44	8	26
3.67	15	47	8	27
3.68	17	50	9	28
3.69	18	51	10	30
3.70	21	51	12	32
3.71	24	52	12	35
3.72	24	53	15	36
3.73	25	55	15	38
3.74	25	56	17	42
3.75	25	57	18	45
3.76	27	60	19	46
3.77	29	63	20	48
3.78	29	63	21	49
3.79	30	64	22	49
3.80	30	65	24	50
3.81	31	66	26	51
3.82	33	66	27	52
3.83	38	67	27	53
3.84	40	68	27	56
3.85	42	68	28	57
3.86	43	69	29	61
3.87	45	69	32	63
3.88	46	70	33	63
3.89	47	70	34	63
3.90	49	72	36	64

Table 4.5 Relationship between the Current and Correlation Methods before Repairs (All)

# FOUND	US290L1A			US290L2A			US290R1A			US290R2A		
SI	C=N	C>N	C<N	C=N	C>N	C<N	C=N	C>N	C<N	C=N	C>N	C<N
3.60	3	12	0	6	27	2	1	8	1	3	17	1
3.61	3	12	0	6	27	2	1	8	2	3	17	1
3.62	3	12	0	6	27	4	1	8	2	4	16	1
3.63	3	12	1	8	25	5	1	8	2	5	15	1
3.64	3	12	1	9	24	7	1	8	2	5	15	1
3.65	3	12	1	9	24	7	1	8	2	5	15	1
3.66	3	12	1	9	24	9	1	8	2	7	13	1
3.67	3	12	3	9	24	9	1	8	3	7	13	1
3.68	3	12	4	9	24	9	1	8	3	7	13	1
3.69	3	12	4	9	24	9	3	6	3	7	13	2
3.70	3	12	5	10	23	10	3	6	4	8	12	2
3.71	3	12	5	12	21	10	3	6	4	9	11	3
3.72	3	12	6	15	18	10	3	6	5	10	10	3
3.73	3	12	7	15	18	10	3	6	7	10	10	3
3.74	3	12	8	16	17	13	3	6	7	12	8	3
3.75	5	10	10	18	15	15	3	6	7	12	8	4
3.76	5	10	12	18	15	17	3	6	8	13	7	4
3.77	6	9	12	19	14	19	3	6	9	13	7	4
3.78	6	9	12	19	14	21	3	6	9	13	7	4
3.79	6	9	15	19	14	23	3	6	10	14	6	4
3.80	6	9	15	20	13	24	3	6	10	14	6	4
3.81	6	9	17	20	13	25	3	6	11	14	6	5
3.82	6	9	20	20	13	26	3	6	11	15	5	5
3.83	6	9	20	21	12	26	3	6	11	15	5	7
3.84	6	9	20	22	11	27	3	6	11	15	5	8
3.85	6	9	21	24	9	28	3	6	11	15	5	10
3.86	6	9	21	24	9	28	3	6	12	15	5	11
3.87	6	9	21	24	9	29	4	5	16	15	5	13
3.88	6	9	22	24	9	29	4	5	17	16	4	15
3.89	6	9	25	24	9	30	4	5	17	16	4	17
3.90	6	9	26	24	9	31	4	5	18	16	4	18

Table 4.6 Relationship between the Current and Correlation Methods after Repairs (All)

# FOUND	US290L1B			US290L2B			US290R1B			US290R2B		
SI	C=N	C>N	C<N	C=N	C>N	C<N	C=N	C>N	C<N	C=N	C>N	C<N
3.60	3	9	6	11	12	21	2	5	3	15	9	5
3.61	3	9	6	11	12	22	2	5	5	15	9	5
3.62	3	9	6	11	12	24	2	5	5	16	8	6
3.63	3	9	9	12	11	24	2	5	5	16	8	7
3.64	3	9	10	13	10	27	2	5	6	16	8	8
3.65	3	9	10	13	10	31	2	5	6	16	8	10
3.66	4	8	11	13	10	31	2	5	6	16	8	10
3.67	4	8	11	13	10	34	2	5	6	16	8	11
3.68	4	8	13	13	10	37	2	5	7	16	8	12
3.69	4	8	14	13	10	38	2	5	8	16	8	14
3.70	4	8	17	13	10	38	2	5	10	16	8	17
3.71	4	8	18	13	10	39	2	5	10	16	8	20
3.72	5	7	19	14	9	39	2	5	13	16	8	21
3.73	6	6	20	14	9	41	2	5	13	17	7	22
3.74	6	6	20	14	9	42	2	5	15	18	6	25
3.75	6	6	20	14	9	43	2	5	16	19	5	27
3.76	6	6	22	16	7	44	2	5	17	19	5	28
3.77	6	6	24	16	7	47	2	5	18	19	5	30
3.78	6	6	24	16	7	47	2	5	19	19	5	31
3.79	6	6	25	17	6	47	2	5	20	19	5	31
3.80	6	6	25	17	6	48	2	5	22	19	5	32
3.81	6	6	26	18	5	48	2	5	24	19	5	33
3.82	6	6	28	18	5	48	2	5	25	19	5	34
3.83	6	6	33	18	5	49	2	5	25	19	5	35
3.84	6	6	35	18	5	50	2	5	25	19	5	38
3.85	6	6	37	18	5	50	2	5	26	19	5	39
3.86	6	6	38	18	5	51	3	4	26	21	3	41
3.87	6	6	40	18	5	52	3	4	29	21	3	43
3.88	6	6	41	18	5	53	3	4	30	21	3	43
3.89	6	6	42	18	5	53	3	4	31	21	3	43
3.90	6	6	44	18	5	55	3	4	33	21	3	44

Table 4.7 Number of Bumps for each 0.1 mile Section before Corrections (Non-Overlapping)

	Lane			
PSI	L1A	L2A	R1A	R2A
3.60	2	5	2	2
3.61	2	6	3	2
3.62	2	6	3	2
3.63	2	6	3	2
3.64	2	6	3	2
3.65	2	6	3	2
3.66	2	6	3	3
3.67	2	6	4	3
3.68	2	6	4	3
3.69	2	6	4	4
3.70	3	7	4	4
3.71	3	7	4	5
3.72	3	7	5	5
3.73	3	8	5	5
3.74	4	8	5	6
3.75	4	8	5	6
3.76	4	8	5	6
3.77	4	8	5	6
3.78	4	8	5	6
3.79	4	8	6	7
3.80	4	8	6	7
3.81	4	8	6	7
3.82	5	8	6	7
3.83	5	8	6	8
3.84	5	8	6	8
3.85	5	8	6	8
3.86	5	8	6	9
3.87	5	8	7	9
3.88	6	8	8	10
3.89	6	8	8	11
3.90	6	8	8	11

Table 4.8 Number of Bumps for each 0.1 mile Section after Corrections (Non-Overlapping)

	Lane			
PSI	L1B	L2B	R1B	R2B
3.60	3	8	4	7
3.61	3	9	4	7
3.62	3	9	4	7
3.63	3	9	4	8
3.64	3	9	4	8
3.65	3	10	4	8
3.66	3	11	4	8
3.67	3	11	4	8
3.68	5	11	4	8
3.69	5	11	4	8
3.70	6	12	5	8
3.71	6	12	5	9
3.72	6	12	6	10
3.73	7	12	6	10
3.74	7	13	6	11
3.75	7	14	6	11
3.76	8	14	7	11
3.77	8	14	7	11
3.78	8	14	7	11
3.79	9	14	7	11
3.80	9	14	7	11
3.81	9	15	7	11
3.82	9	16	7	11
3.83	10	16	7	11
3.84	10	16	7	11
3.85	10	16	8	11
3.86	10	16	8	11
3.87	11	16	10	11
3.88	11	16	10	11
3.89	12	16	10	11
3.90	12	16	10	11

Table 4.9 Relationship between the Current and Correlation Methods before Repairs (Non-Overlapping)

# FOUND	US290L1A			US290L2A			US290R1A			US290R2A		
SI	C=N	C>N	C<N	C=N	C>N	C<N	C=N	C>N	C<N	C=N	C>N	C<N
3.60	2	13	0	3	30	2	1	8	1	1	19	1
3.61	2	13	0	3	30	2	1	8	2	1	19	1
3.62	2	13	0	3	30	3	1	8	2	1	19	1
3.63	2	13	0	3	30	3	1	8	2	1	19	1
3.64	2	13	0	3	30	3	1	8	2	1	19	1
3.65	2	13	0	3	30	3	1	8	2	1	19	1
3.66	2	13	0	3	30	3	1	8	2	2	18	1
3.67	2	13	0	3	30	3	1	8	3	2	18	1
3.68	2	13	0	3	30	3	1	8	3	2	18	1
3.69	2	13	0	3	30	3	1	8	3	2	18	2
3.70	2	13	1	3	30	3	1	8	3	2	18	2
3.71	2	13	1	3	30	3	1	8	3	2	18	3
3.72	2	13	1	4	29	3	1	8	4	2	18	3
3.73	2	13	1	4	29	3	1	8	4	2	18	3
3.74	2	13	2	4	29	3	1	8	4	3	17	3
3.75	2	13	2	4	29	4	1	8	4	3	17	3
3.76	2	13	2	4	29	4	1	8	4	3	17	3
3.77	2	13	2	4	29	4	1	8	4	3	17	3
3.78	2	13	2	4	29	4	1	8	4	3	17	3
3.79	2	13	2	4	29	4	1	8	5	4	16	3
3.80	2	13	2	4	29	4	1	8	5	4	16	3
3.81	2	13	2	4	29	4	1	8	5	4	16	3
3.82	2	13	3	4	29	4	1	8	5	4	16	3
3.83	2	13	3	4	29	4	1	8	5	4	16	4
3.84	2	13	3	4	29	4	1	8	5	4	16	4
3.85	2	13	3	4	29	4	1	8	5	4	16	4
3.86	2	13	3	4	29	4	1	8	5	4	16	5
3.87	2	13	3	4	29	4	1	8	6	4	16	5
3.88	2	13	4	4	29	4	1	8	7	5	15	5
3.89	2	13	4	4	29	4	1	8	7	5	15	6
3.90	2	13	4	4	29	4	1	8	7	5	15	6

Table 4.10 Relationship between the Current and Correlation Methods after Repairs (Non-Overlapping)

# FOUND	US290L1B			US290L2B			US290R1B			US290R2B		
SI	C=N	C>N	C<N	C=N	C>N	C<N	C=N	C>N	C<N	C=N	C>N	C<N
3.60	1	11	2	6	17	2	2	5	2	5	19	2
3.61	1	11	2	6	17	3	2	5	2	5	19	2
3.62	1	11	2	6	17	3	2	5	2	5	19	2
3.63	1	11	2	6	17	3	2	5	2	5	19	3
3.64	1	11	2	6	17	3	2	5	2	5	19	3
3.65	1	11	2	6	17	4	2	5	2	5	19	3
3.66	1	11	2	6	17	5	2	5	2	5	19	3
3.67	1	11	2	6	17	5	2	5	2	5	19	3
3.68	1	11	4	6	17	5	2	5	2	5	19	3
3.69	1	11	4	6	17	5	2	5	3	5	19	3
3.70	1	11	5	6	17	6	2	5	3	5	19	3
3.71	1	11	5	6	17	6	2	5	4	5	19	4
3.72	1	11	5	6	17	6	2	5	4	5	19	5
3.73	2	10	5	6	17	6	2	5	4	5	19	5
3.74	2	10	5	6	17	7	2	5	4	6	18	5
3.75	2	10	5	6	17	8	2	5	5	6	18	5
3.76	2	10	6	6	17	8	2	5	5	6	18	5
3.77	2	10	6	6	17	8	2	5	5	6	18	5
3.78	2	10	6	6	17	8	2	5	5	6	18	5
3.79	2	10	7	6	17	8	2	5	5	6	18	5
3.80	2	10	7	6	17	8	2	5	5	6	18	5
3.81	2	10	7	6	17	9	2	5	5	6	18	5
3.82	2	10	7	7	16	9	2	5	5	6	18	5
3.83	2	10	8	7	16	9	2	5	5	6	18	5
3.84	2	10	8	7	16	9	2	5	6	6	18	5
3.85	2	10	8	7	16	9	2	5	6	6	18	5
3.86	2	10	8	7	16	9	2	5	8	6	18	5
3.87	2	10	9	7	16	9	2	5	8	6	18	5
3.88	2	10	9	7	16	9	2	5	8	6	18	5
3.89	2	10	10	7	16	9	2	5	8	6	18	5
3.90	2	10	10	7	16	9	2	5	8	6	18	5

Chapter 5

Summary and Recommendations

5.1 Summary

This report presented a procedure for detecting defects using road profile data collected with inertial profilers. In the method developed, bumps or dips are identified by cross correlating the first derivatives of several bump templates with the first derivative of the measured profile of a section under evaluation. Bump templates were established based on an evaluation of several artificial bumps fabricated at TTI. From this evaluation, researchers selected a "golden" bump to establish templates for cross correlation by varying the wavelength and amplitude of the "golden" bump profile. The proposed method is referred to as the Template Analysis Procedure, or TAP.

TAP is based on the new ride equation developed in TxDOT Project 0-4901. Application of this new equation to compute SIs from profile data collected on the Austin control sections demonstrated the sensitivity of the new SI to the presence of localized roughness. Further investigations of the effects of simulated bumps on various ride statistics revealed that the new SI is affected by both the amplitude and wavelength of a bump. In contrast, the current SI and IRI were found to be sensitive only to the bump amplitude for the range of simulated bumps considered in the analysis. Thus, this project investigated the application of the new ride model for detecting bumps and dips, resulting in the development of a new method based on cross correlation.

In this method, the new SI is used to establish the need for evaluating localized roughness on a given section. The engineer specifies an acceptable NSI for a given project. For sections where the new SIs are equal to or greater than this threshold, no evaluation of localized roughness is performed since the ride is deemed acceptable from a road user perspective. However, for sections where the new SIs are lower than the threshold, TAP is used to locate defects within those sections. This evaluation is accomplished by cross correlating bump templates with the measured profile and using a threshold correlation coefficient to identify defects. More

specifically, if the magnitude of the correlation between a particular profile feature and the bump template is at or above the threshold value, that particular feature is identified as a defect in the proposed method.

The threshold correlation coefficient is critical to the success of detecting defects using TAP. In this report, researchers illustrated a method for determining the threshold based on the acceptable NSI specified by the engineer. This method is based on evaluating the correlation coefficients for an unbiased sample of 0.1 mile pavements having new SIs greater than or equal to the acceptable value. Specifically, the measured profiles on these sections are used to estimate the expected value of the distribution of the maximum correlation coefficients and its variance. These estimates are then used in equation 3.1 to determine the correlation threshold corresponding to the acceptable level of the new SI specified by the engineer.

Researchers evaluated the template analysis procedure using profile data collected on a rehabilitation project along US 290 near Brenham. From this evaluation, the following findings are noted:

- The number of defects detected using TAP increases with the acceptable level of NSI for the range of threshold values considered in the analysis (3.6 to 3.9). This result is to be expected since more sections are evaluated as the threshold NSI increases.
- If all defects detected are counted, TAP yielded more defects than SS 5880 for the same profile data. However, the new method yielded fewer defects than SS 5880 if each set of overlapping bumps or dips is counted as one occurrence.

5.2 Recommendations

Because of the one-year duration of this study, it was not possible to compare TAP with the current ride specifications on additional projects. To determine the potential impact of the proposed method to current practice, additional shadow testing on other rehabilitation projects is needed. In addition, the following recommendations are offered:

- The threshold correlation coefficient in this report was determined based on an acceptable new SI of 4.0. In practice, this criterion will likely vary, depending on the acceptable level of NSI. For implementation purposes, a

table of recommended threshold correlation coefficients for different acceptable levels of NSI should be developed.

- The practical utility of the TAP program would be enhanced if a function is included that would estimate how the NSI would change as specific bumps or dips are taken out. In this way, the engineer can identify the corrections that are predicted to provide the most improvement in the ride quality of a given project.

REFERENCES

1. Fernando, E. G., and Bertrand, C. *Application of Profile Data to Detect Localized Roughness*. Transportation Research Record 1813, Transportation Research Board, Washington, D. C., 2002, pp. 55 – 61.

2. Fernando, E. G., and Leong, S. C. *Profile Equipment Evaluation*. Research Report 1378-2, Texas Transportation Institute, Texas A&M University, College Station, Texas, 1997.

3. Ifeachor, Emmanuel C., Jervis, Barrie W. *Digital Signal Processing: A Practical Approach*, Second Edition, Prentice Hall, 2002

4. National Quality Initiative Steering Committee. *National Highway User Survey*. Coopers & Lybrand and the Opinion Research Corporation, May 1996.

5. Sayers, M. W. *On the Calculation of International Roughness Index from Longitudinal Road Profile.* Transportation Research Record 1501, Transportation Research Board, Washington, D.C., 1995, pp. 1 – 12.

6. Walker, R. S., and Fernando, E. G. *Evaluation of Ride Equation*. Research Report 4901-1F, The University of Texas at Arlington and the Texas Transportation Institute, July 2002.

7.

APPENDIX:
Profile Data Collection
To Support Development Work

Project 0-4479 aimed to develop an improved methodology for evaluating localized roughness that considers road user perception of ride quality and uses inertial reference profile measurements to detect profile wavelengths and amplitudes detrimental to ride. To support this development work, the project director sent out a survey to identify rehabilitation projects where the districts executed change orders to implement SS5880/5440 for quality assurance testing of initial pavement smoothness. Table A1 identifies district projects where change orders were executed, based on the survey results. All projects listed involved rehabilitation of flexible pavements. No Portland cement concrete (PCC) projects were found where change orders to the new ride specification were made, nor were upcoming PCC projects identified where SS5880/5440 was to be used.

From communications with the districts or contractors responsible for quality assurance testing, the project director and researchers obtained profile data from the Abilene, Atlanta, Lufkin, Lubbock, Pharr, Tyler, and Yoakum projects. Using TxDOT's Ride Quality program, which implements the bump detection methodology incorporated in SS5880/5440 and Item 585, researchers determined the occurrences of bumps or dips on these projects. Table A2 summarizes the number of defects determined from the program, while Tables A3 to A9 give the defect locations. Researchers initially planned to use the data from these projects to establish threshold levels for identifying localized roughness using the template analysis method. Specifically, threshold levels for the following criteria are required:

1. critical PSI value that would trigger an evaluation of localized roughness on a 0.1-mile section using the template analysis method; and
2. the magnitude of the correlation between the defect template and surface profile for identifying bumps or dips in the profile.

By comparing the results from the template analysis with those from TxDOT's Ride Quality program, threshold values for the above criteria can be determined. However, while this approach would yield criteria that are reasonable relative to current practice, it will not provide an independent verification or calibration of the proposed methodology. Consequently, a different approach was considered in a meeting held in April 2003 with the TxDOT project monitoring committee. In that meeting, the committee proposed that researchers identify projects where fine milling or other repairs are planned to remove existing roughness. The intent is to measure the surface profiles before and after repairs to establish the locations of defects.

Researchers identified a suitable project along US 290 in the Bryan District where the existing asphalt concrete pavement was resurfaced. This project began at the junction of US 290 and SH 36 in Brenham and proceeded westward for about 12 miles (see Figure A1). The project was let under the straightedge specification, and had numerous defects along its length as determined from the straightedge.

The Bryan District provided surface profile measurements taken on the travel lanes before the contractor undertook repairs on the project. After repairs, surface profiles were again measured using an inertial profiler from the Materials and Pavements Section of TxDOT's Construction Division. The contractor ground out the bumps at the locations determined from the straightedge. To tie in these locations to the profile measurements, researchers surveyed the project with an instrumented van with a camera setup that permitted photos of the corrected areas to be taken as the van was driven along the travel lane. Figures A2 to A5 show pictures of some of the repaired areas along the project. As each of these areas came into view, researchers took a photograph using a notebook computer that was hooked up to the camera and the distance-measuring instrument (DMI) of the vehicle. A computer program automatically saved each photograph to a file with a name that corresponds to the traveled distance along the lane when the picture was taken. In this way, researchers established the locations where the contractor undertook repairs along the project to take out defects identified by the engineer and the contractor using the straightedge. Table A10 summarizes the locations of these corrections. This information was used to evaluate the template analysis procedure in Chapter 4 of this report.

Table A.1 District Projects Change-Ordered to SS5880

District	County	Highway	CSJ	Project limits (reference markers)	
				From	To
Abilene	Nolan	IH20	6-2-92	0229 -00.065	0235 +00.200
Atlanta	Upshur	SH300			
Bryan	Brazos	SH47			
Bryan	Waller	SH75			
Bryan	Washington	US290	0114-09-062	0656 +00.341	0658 +01.646
Lubbock	Dawson	SH137			
Lufkin	Polk	SH146	0388-01-038		
Pharr	Hidalgo	US83			
Tyler	Gregg	IH20	0495007-052	0586 +00.854	0593 +00.200
Yoakum	Jackson	US59	0089-05-042		

Table A.2 Number of Defects Based on SS5880

Project	Length (miles)	Number of defects
IH20 Abilene	6.3	21
SH300 Atlanta	4.4	10
SH 137 Lubbock	18.5	57
SH146 Lufkin	4.8	6
US83 Pharr	4.3	19
IH20 Tyler	6.4	3
US59 Yoakum	4.7	8

Table A.3 Defect Locations along Abilene Project

Lane	Reference marker	Type of defect
L1	0229 +00.329	Bump
	0226 +00.393	Bump
	0226 +00.392	Bump
	0226 +00.390	Dip
	0226 +00.203	Dip
	0226 +00.156	Dip
	0226 +00.155	Dip
	0226 +00.154	Bump
	0226 +00.152	Dip
	0226 +00.102	Bump
L2	0224 +00.952	Bump
	0224 +00.913	Bump
	0224 +00.911	Dip
	0223 +00.656	Dip
	0221 +00.578	Bump
	0221 +00.576	Dip
	0221 +00.154	Dip
	0221 +00.152	Bump
	0221 +00.149	Bump
	0221 +00.148	Dip
	0220 +00.348	Dip

Table A.4 Defect Locations along Atlanta Project

Lane	Reference marker	Type of defect
K1	0269 +00.034	Dip
	0269 +00.035	Bump
	0269 +00.036	Bump
	0269 +00.362	Dip
K2	0266 +00.941	Dip
	0267 +00.383	Dip
	0267 +00.998	Bump
	0269 +00.525	Bump
	0270 +00.990	Dip
K6	0266 +00.249	Dip

Table A.5 Defect Locations along Lubbock Project

Lane	Reference marker	Type of defect
K1	0258 +00.003	Bump
	0258 +00.463	Dip
	0258 +00.497	Dip
	0258 +00.512	Bump
	0258 +00.526	Bump
	0259 +00.234	Dip
	0259 +00.247	Dip
	0259 +00.247	Dip
	0259 +00.572	Dip
	0260 +00.156	Bump
	0260 +00.228	Bump
	0260 +00.229	Bump
	0260 +00.259	Bump
	0260 +00.260	Bump
	0260 +00.378	Dip
	0260 +00.692	Dip
	0260 +00.700	Dip
	0260 +00.700	Dip
	0262 +00.348	Dip
	0262 +00.655	Dip
	0262 +00.855	Dip
	0268 +00.436	Bump
	0270 +00.620	Bump
	0270 +00.621	Bump
	0270 +00.699	Bump
	0275 +00.437	Bump
	0275 +00.439	Dip
	0275 +00.440	Dip
	0275 +00.905	Bump

Lane	Reference marker	Type of defect
	0275 +00.908	Dip
	0275 +00.908	Dip
	0276 +00.291	Bump
	0276 +00.484	Dip
K2	0276 +00.486	Dip
K6	0276 +00.341	Dip
	0276 +00.307	Dip
	0276 +00.244	Dip
	0276 +00.119	Dip
	0276 +00.048	Bump
	0275 +00.857	Bump
	0275 +00.545	Bump
	0275 +00.530	Bump
	0275 +00.527	Dip
	0275 +00.525	Bump
	0275 +00.523	Dip
	0270 +00.865	Dip
	0263 +00.850	Bump
	0263 +00.429	Bump
	0260 +00.044	Bump
	0259 +00.917	Bump
	0259 +00.915	Dip
K7	0276 +00.493	Dip
	0275 +00.823	Bump
	0275 +00.822	Dip
	0275 +00.714	Dip
	0275 +00.714	Dip
	0275 +00.705	Dip

Table A.6 Defect Locations along Lufkin Project

Lane	Station	Type of defect
K1[A]	0004+05.0	Bump
	0004+19.0	Dip
	0006+30.5	Bump
	0057+64.0	Bump
K6[B]	2397+92.3	Dip
	2397+97.8	Bump

[A] Beginning station for K1 lane is 0000+00.0

[B] Beginning station for K6 lane is 2548+12.8

Table A.7 Defect Locations along Pharr Project

Lane	Station[1]	Type of defect
L1	0184+53.2	Bump
	0167+34.3	Bump
L2	0192+20.0	Dip
	0188+99.4	Bump
	0188+78.5	Dip
	0182+16.8	Dip
	0182+05.9	Bump
	0174+67.5	Dip
	0171+21.2	Dip
	0167+24.7	Dip
	0165+91.2	Bump
	0165+90.4	Bump
	0165+82.9	Dip
	0067+15.1	Bump
	0067+14.2	Bump
	0067+04.2	Dip
	0065+75.5	Dip
	0010+20.1	Bump
	0000+06.9	Dip

[1] Beginning station for L1 and L2 lanes is 0225+51.0

Table A.8 Defect Locations along Tyler Project

Lane	Reference marker	Type of defect
R2	0586 +05.353	Dip
L1	0586 +00.980	Dip
L2	0586 +04.599	Dip

Table A.9 Defect Locations along Yoakum Project

Lane	Station[1]	Type of defect
K6	0055+51.5	Bump
	0055+50.0	Bump
	0044+51.5	Bump
	0040+64.0	Bump
K7	0186+75.5	Bump
	0138+84.5	Dip
	0134+97.0	Dip
	0007+28.0	Bump

[1] Beginning station for K6 and K7 lanes is 0188+55.0

Table A.10 Locations of Corrections along US290 Project in Brenham

Distance in feet from start of profile measurements on travel lane									
R1[A]	**R2[A]**	**L1[B]**		**K1[C]**		**K2[C]**	**K6[D]**		**K7[D]**
476	9975	5692	30927	136	6435	387	4333	11546	7386
1268	25405	6230	31004	250	6522	772	4629	11684	7789
4147	42595	8524	31170	453	7703	2976	4755	11881	11129
5349	43450	15567	31450	665	7963	3083	4810	12318	11852
9641		15723	31589	1071	8239	3295	4873	12637	12440
11513		15867	32912	1198	8565	4731	5355	13301	12848
13336		17419	33400	1435	8919	8614	5637	13465	14290
13928		17677	33534	1500	9964	9115	6030	13631	14466
14712		19674	34583	1574	10273	10132	6208	13718	14816
15847		20303	37913	1700	10646		6445	13797	15160
22618		21610	38580	1968	10891		6744	13872	16006
23663		23334	43011	2043	11143		6900	13969	
24058		25478	43247	2142	11421		7176	14014	
24906		25594	43419	2228	11663		7601	14242	
25271		25977	43606	2973	11826		7904	14309	
25323		26132	44499	3301	11947		8285	14543	
26141		26248	47141	3572	12133		8607	14726	
29985		26430	49074	3805	12273		8901	14888	
30175		27531	49588	5608	12453[E]		9352	15210	
				6062	12861[E]		9788	15414	
							9836	15478	
							10126	15654	
							10290	16003	
							11199	16193	

[A] Profile runs on R1 and R2 started about 1.4 miles east of RM 658 and went east for about 9.1 miles

[B] Profile runs on L1 and L2 started about 1.1 miles west of RM 670 and went west for about 9.1 miles

[C] Profile runs on K1 and K2 started about 1.1 miles west of RM 670 and went east for about 3.1 miles

[D] Profile runs on K6 and K7 started at junction of US290 and SH36 and went west for about 3.1 miles

[E] Overlay placed between 12,453 and 12,861 ft on K1 lane

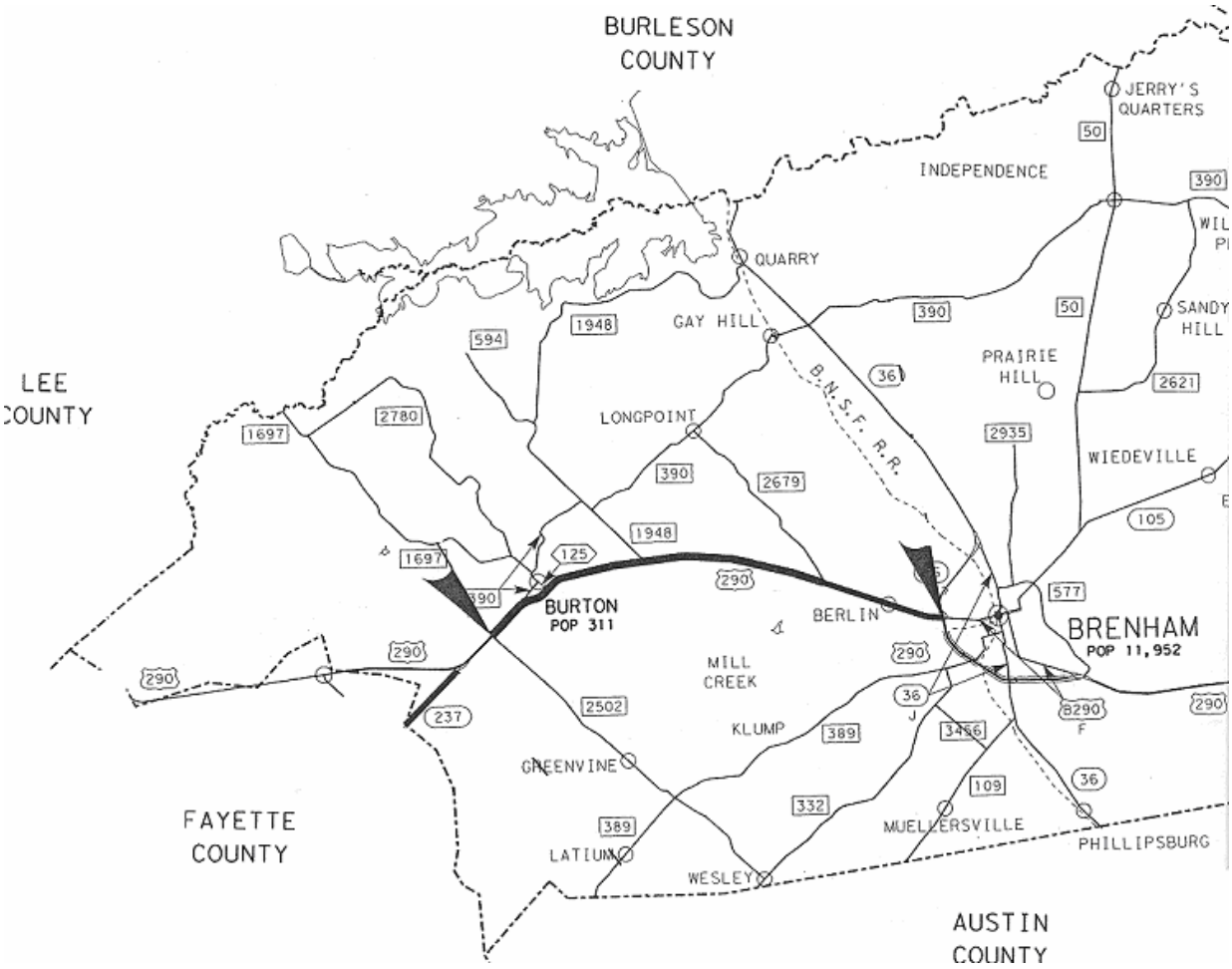

Figure A.1 US290 Project Investigated in Study

Figure A.2 Grind Spots along R1 Lane of US290 about 4147 ft from Start of Profile Survey

Figure A.3 Grind Spots along L1 Lane of US290 about 19,674 ft from Start of Survey

Figure A.4 Beginning of Overlaid Area on K1 Lane about 12,453 ft from Start of Survey

Figure A.5 Grind Spots along K6 Lane of US290 about 14,888 ft from Start of Survey